Real-Time, Label-Free Detection of Biological Entities Using Nanowire-Based FETs

Marco Curreli, Rui Zhang, Fumiaki N. Ishikawa, Hsiao-Kang Chang, Richard J. Cote, Chongwu Zhou, and Mark E. Thompson

(Invited Paper)

***Abstract*—Nanowire (NW)-based FETs are promising devices with potential applications ranging from health monitoring to drug discovery. In fact, these devices have demonstrated the ability to detect a variety of analytes such as particular DNA sequences, cancer biomarkers, and larger entities such as viruses. These sensor devices have also been used to monitor enzymatic activities and study the behavior of potential drug molecules. The detection of the analytes occurs with high specificity and sensitivity in reasonably short time. Here, we review the recent literature produced in the field of NW FET biosensors. We elaborate on the parameters that ultimately influence device performance such as methods of NW production, device dimensionality, and active measurement conditions. Significant progress has been made in this field of technology; however, it is often difficult to compare literature reports due to differences in both measurement conditions and data analysis. The standardization of certain active measurement conditions, such as the ionic strength of the analyte solutions, and manipulation of data are proposed to facilitate comparison between different NW biosensors.**

***Index Terms*—Cancer nanotechnology, FET nanosensor, label-free detection, nanowire (NW) biosensor.**

I. Introduction

In THE PAST 15 years, material scientists and engineers have progressively miniaturized the materials that constitute the building blocks of various biomedical devices [1]–[3]. This progressive downscaling has led to the creation of materials with at least one critical dimension falling within the 1–100 nm range. There are two principal driving forces that promote the exploration of matter in the nanometer range. First, nanomaterials are comparable in size with most biological entities, such as proteins, nucleic acids, cells, viruses, etc. (as shown in Fig. 1), making them the ideal interface materials between biological molecules and scientific instruments. Second, this new class of materials possesses unique physical and chemical properties directly arising from their size such as their high surface-to-volume ratio (S/V). A direct consequence of this high S/V ratio is that a large fraction of the atoms in the material are located at or near the surface. This proximity causes the surface atoms to play an important role in determining the physical, chemical, and particularly electronic properties of the nanomaterials. This dependence on the properties of the nanomaterial/surrounding interface makes nanomaterials excellent substrates for molecular sensing applications.

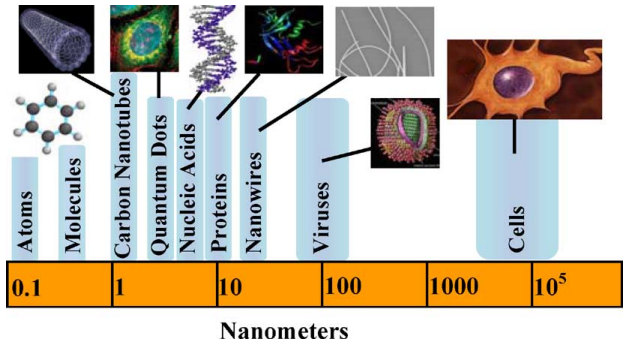

Fig. 1. Size of several nanomaterials is compared to the size of some biological entities, such as nucleic acids, proteins, virus, and cells.

A diversity of sensor architectures has been designed and fabricated during the last decade that utilizes different nanomaterials as a sensing element (cantilevers, quantum dots, nanotubes, nanowires (NWs), nanobelts, nanogaps, and nanoscale films) [4]–[17]. Some of these sensing devices, such as those based on cantilevers and quantum dots, are highly specific, ultrasensitive, and have short response times. However, these devices require integration with optical components in order to translate surface-binding phenomena into a readable signal. The need for detection optics is expected to significantly increase the cost of operation for such a device. In contrast, sensors designed to operate like FET can directly translate the analyte–surface interaction into a readable signal, without the need for elaborate optical components. These devices utilize the electronic properties of the sensing element, such as its conductance, to produce the signal output. Sensors based on FETs promise to revolutionize bioanalytical research by offering the direct, real-time, highly specific, ultrasensitive, and label-free detection of the desired biomolecule [18]–[21].

A number of reviews have appeared recently on the use of carbon nanotube (CNT)-based devices for biosensing [22]–[25]. While we will discuss some of the properties of CNT-based devices for comparative purposes, this review will focus on

Manuscript received May 9, 2008; revised September 3, 2008; accepted September 8, 2008. First published September 26, 2008; current version published December 24, 2008. The review of this paper was arranged by Associate Editor R. Lake.

M. Curreli, R. Zhang, and M. E. Thompson are with the Department of Chemistry, University of Southern California, Los Angeles, CA 90089 USA (e-mail: mthompso@usc.edu).

F. N. Ishikawa, H.-K. Chang, and C. Zhou are with the Department of Electrical Engineering, University of Southern California, Los Angeles, CA 90089 USA.

R. J. Cote is with the Department of Pathology, University of Southern California, Los Angeles, CA 90033 USA.

Color versions of one or more of the figures in this paper are available online at http://ieeexplore.ieee.org.

Digital Object Identifier 10.1109/TNANO.2008.2006165

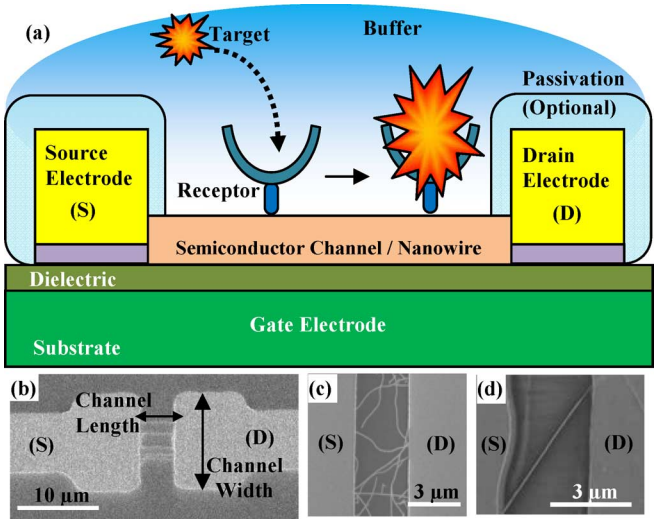

Fig. 2. Structure of an FET nanobiosensor. (a) Cross-sectional view: source and drain electrodes bridge the semiconductor channel. The gate electrode can be used to modulate the conductivity of the semiconductor channel. A receptor molecule attached to the surface of the semiconductor material can specifically recognize and capture a target molecule from a buffer solution. (b) Top view: SEM image of a typical nano-FET. In these structures, the channel length is the S–D distance and the channel width is the S or D electrode width. Examples of nano-FET fabricated at the author's research facility using either (c) carbon nanotubes or (d) indium oxide NWs as semiconductor materials.

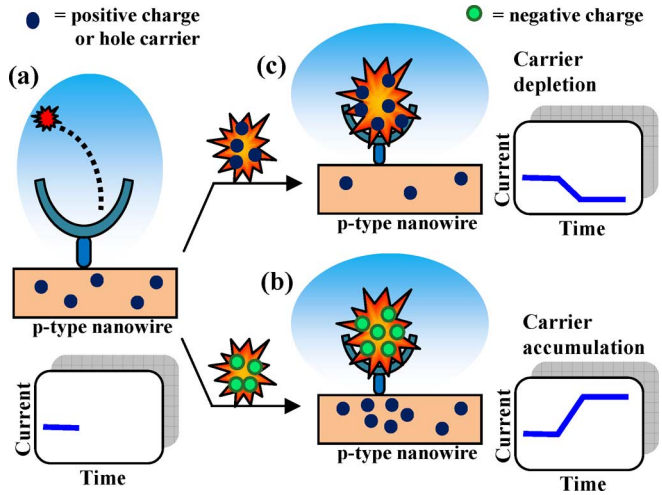

Fig. 3. Mechanism to modulate the conductance of a p-type NW FET. (a) NW exhibits uniform conductance prior to any interaction with the target molecule. (b) When a negatively charged target molecule binds to the receptor, it attracts positive hole carriers in the region of the wire below the receptor. This attraction causes carriers to accumulate resulting in an increase in conductance. (c) On the other hand, when a positively charged target molecule is captured, it depletes the carrier density in the NW causing a decrease in conductance.

the use of FETs fabricated using semiconductor NWs (e.g., Si, In_2O_3) for detection of biological molecules.

II. FET Nanobiosensors

An FET sensor has the structure of a common three-electrode transistor, where the source and drain electrodes bridge the semiconductor channel and the gate electrode modulates the channel conductance. The typical structure of an FET sensor is illustrated in Fig. 2(a). In the case of FET nanosensors, the semiconductor channel is made of a nanomaterial and is used as the "sensing" component of the device. Semiconductor channels can be fabricated using several nanomaterials, including CNTs and NWs. In order to provide selectivity toward a unique analyte, a specific recognition group (also called a receptor, ligand, or probe) is anchored to the surface of the semiconductor channel. This receptor is typically chosen to recognize its target molecule (also called analyte) with a high degree of both specificity and affinity.

FET sensors can be subdivided into three main groups depending on the type of receptor used for the analyte recognition and on how this signal is generated [26]:

1) enzyme-modified FETs, usually involving the product of a catalytic reaction (e.g., H^+ or H_2O_2 generation or a reaction between an enzyme and its substrate);
2) cell-based FETs, utilizing potential changes that are produced by living biological systems;
3) immunologically modified FETs and DNA-modified FETs, exploiting surface polarization effects or changes in the dipole moment (e.g., antigen–antibody binding or DNA hybridization).

For immunological- and DNA-modified FET sensors, the semiconductor channel has a uniform conductance determined by the main carrier density in the NW (holes for a p-type semiconductor or electrons for an n-type semiconductor). The carrier density in the NW is proportional to the conductance of the wire, which can be determined from the source–drain current of the device. The current measured for the device at fixed potentials for both source–drain and gate electrodes is constant over time, as illustrated schematically in Fig. 3(a) for a p-type NW. Any change in the current can be related to a change in conductance of the NW. When a charged analyte molecule binds to a receptor anchored on the NW, an electric field created on the surface exerts an effect both inside and outside the semiconductor channel [27]. If the bound analyte molecule carries a charge opposite to the main carriers in the FET, then charge carriers will accumulate under the bound analyte, thus causing an increase in the device conductivity. This mechanism is shown in Fig. 3(b), where a negatively charged molecule such as DNA binds to the p-type NW, causing a buildup of hole carriers, thus resulting in an increase in conductivity. In contrast, analytes with molecular charges same as that of the main carriers in the FET lead to depletion of main carriers beneath the bound analyte, causing a decrease in conductivity. The latter case is shown in Fig. 3(c), where a positively charged molecule, such as a protein below its isoelectric point (pI), depletes the carriers upon binding to the NWs.

A. CNT-Based FET Biosensors

FET-sensors-based single-walled carbon nanotubes (SWNT) have been reviewed recently [22]–[25]. In this section, we highlight some key concepts of CNT FETs and summarize the advantages and disadvantages of such a platform. CNTs could be considered an ideal material for sensing applications because every atom in an SWNT is located on the surface, leading to extreme sensitivity to the surrounding environment. Surface-modified CNTs are compatible (nontoxic) with living organisms such as cells [28]–[32], thus providing the appropriate interface between biological entities and electronic circuits. Also, nanotubes can be readily synthesized from inexpensive precursors,

such as methane, or purchased from commercial sources with high purity.

The mechanism leading to signal transduction in an SWNT biosensor has, until recently, been poorly understood. For example, several studies have reported that an SWNT device will show a decrease in resistance for every protein tested, independent of the overall charge on the protein [33], [34]. This observation conflicts with that made on NW-based transistors [35], [36], and cannot be explained as an electrostatic gating effect caused by the charged analyte perturbing the nanotube carriers. The key to resolve this discrepancy was first proposed by Chen *et al.* [33]. They suggested that the dominant sensing mechanism is a modulation of the Schottky barrier at the electrodes–nanotube interface caused by binding of the analyte and the receptor. This proposal has received support from other groups [37], [38], whereas Heller *et al.* observed that another sensing mechanism, electrostatic gating, can also play an important role depending on the nature of the analyte [37].

Unfortunately, SWNTs suffer from major drawbacks in sensing applications. These drawbacks include the need to separate semiconducting nanotubes from metallic nanotubes and a nonuniform distribution of bandgaps that leads to an inability to fine-tune the electronic properties. Long-term, water-stable modification with bioreceptor molecules has proved to be a challenge. Regardless, CNTs have been shown to be able to detect proteins, oligonucleotides, and enzymatic activities with high sensitivity and specificity.

B. NW-Based FET Biosensors

Semiconductor NW FET biosensors are currently the focus of intense research [39]. NWs can be manufactured with high reproducibility, offer a well-understood surface chemistry, and provide the possibility of fine-tuning the conductivity via introduction of dopants. Semiconducting NWs can be prepared with a variety of semiconducting materials such as Si, Ge, or metal oxides (e.g., In_2O_3, SnO_2, ZnO, etc.), which are potentially useful in sensing applications. The balance of this review will discuss the fabrication of Si- and In_2O_3-based NWs (the only materials used to date in NW FET-based biosensors), their incorporation into FETs, and the use of these devices in biosensing. The performance of these devices is summarized in Table I.

III. NW Production Methods

Several fabrication methods have been used to produce semiconducting NWs for use in FET biosensors, and will be described in the following section. NWs can be prepared with very different dimensions, carrier densities, and mobilities, which can substantially affect the performance of the sensor device. Several studies have been carried out in order to elucidate the dependence of device characteristics on NW dimensions and doping. For instance, Elfstrom *et al.* compared the electrical characteristics of Si NW-based FETs upon exposure of the device to buffer solutions of different pH and as a function of the Si NW diameter (50–170 nm) [40]. It was found that environmental effects on the NW FET properties decrease with increasing NW diameter, such that wires larger than 150 nm behave similarly to those with micrometer-sized diameter. A similar conclusion was reached by Stern *et al.* when devices fabricated using smaller NWs showed greater sensitivity to pH variation than larger NWs [35]. The device sensitivity dependence on the channel dimensions and doping concentration was also demonstrated in other studies (see later) [41], [42]. These studies underscore the importance for small dimensions in order to achieve high levels of sensitivity to the environment necessary to detect the effects brought about by analyte binding.

Several NW characteristics that can be altered during NW preparation, such as NW dimension and doping levels, have been shown by Nair and Alam to control device performance [43]–[45]. Their simulations indicate that devices fabricated using small-diameter NWs (about 10 nm or less) would decrease the minimum amount of analytes required for a detectable signal. Their paper also indicates that for nanobiosensors (NW sensors operating in high-dielectric, aqueous buffers), the doping density determines the device sensitivity, not the doping type (n- or p-type). Lightly doped NWs are expected to exhibit greater sensitivity than highly doped or undoped devices, as experimentally demonstrated by Kim *et al.* [42] and noted by Cui *et al.* [36]. However, fabricating sensor devices with very small diameter NWs and very low doping concentration could introduce significant variability from device to device in a large array [45].

A. Top-Down Technology

Top-down fabrication technologies start with bulk materials and reduce the material dimensions using various techniques to cut, pattern, etch, and shape these materials into the desired geometry and order [39]. These top-down techniques can either be e-beam lithography, photolithography combined with size-reducing strategies, such as the self-limiting oxidation, or a "nano-dimension" transfer method such as the superlattice NW pattern transfer (SNAP) method (*vide infra*).

NWs fabricated by top-down techniques are uniform (nearly identical) and well aligned. Top-down methods usually produce NWs in high yields, in a predetermined orientation and position on the substrate, making them easy to integrate into functional devices. Disadvantages of top-down fabrication include high costs and a slow rate of production. Also, NWs produced by top-down technologies can rarely approach the size of CNTs (1–2 nm). However, top-down techniques offer an excellent control over the NW length, which is crucial since the sensitivity is inversely proportional to the length [45]. Top-down production of NWs employs a silicon-on-insulator (SOI) wafer as a substrate. SOI is a three-layer substrate where the bottom, heavily doped Si layer can be used as a gate electrode in the FET. The middle layer, a 50- to 200-nm-thick silicon oxide, constitutes the dielectric in a FET. The Si NWs are etched from a top layer (30–200 nm thick) made of single-crystal silicon. This top layer can be thinned to the desired thickness, typically the approximate thickness of the NWs, using oxidation and wet etching techniques. The Si top layer can also be doped by several techniques in order to produce n-type or p-type NWs. Presently, this technique has been used to fabricate only Si NWs because of

TABLE I
DEVICE SPECIFICATIONS AND DETECTION PARAMETERS FOR NW FET

Entry	Device Specifications [a]	Linkers [b]	Capture agent(s) [c]	Analyte(s) [d]	Solution Delivery [e]	Media [f]	Ionic strength [g]	Apprx. λ_D (nm) [h]	pH	Performance [i] / Detection Limits	Ref. # Group
1	B; p-Si, n-Si; (d=20); Pass: Si_3N_4	APTMS	Anti-PSA Anti-CEA Anti- Mucin-1	PSA CEA Mucin-1	Microfluidic	Phosphate	6 μM	130	7.4	PSA: 2 fM CEA: 0.55 fM Muc-1: 0.49 fM	[21] Lieber
			Anti-PSA	PSA		Desalted serum	N/A	N/A	N/A	26 fM	
			ssDNA*	Telomerase		HEPES	4.5 μM	150		Extract from 10 HeLa cells	
2	B; p-Si (d=20)	APTMS	Anti-tyrosine kinase Abl	ATP	Microfluidic Pass: PEG	HEPES	4.5 μM	150	7.5	100 pM	[60] Lieber
3	B; p-Si (d=20) Pass: Si_3N_4	APTMS	Anti-hemagglutinin	Influenza A virus	Microfluidic	Phosphate	50 μM	45	6.0	Single virus	[61] Lieber
4	B; p-Si (d=20)	Biotinyl/ Avidin	ssPNA	ssDNA	Microfluidic	N/A	N/A	N/A	N/A	10 fM	[62] Lieber
5	B; p-type Si (d=20)	APTES	Biotin	Streptavidin	Microfluidic	Phosphate	9 mM	3.4	9	10 pM	[36] Lieber
				Anti-Biotin		Phosphate	9 mM	3.4	7	10 nM	
6	B; n-In_2O_3 (d=10)	3-PPA	PSA-Ab	PSA	Mixing cell	1x PBS	180 mM	0.75	7.4	140 fM (→7 pM)	[57] Zhou
7	T; p-Si, n-Si (t=40, w=50-150)	NBAD	Biotin	Streptavidin (SA), Avidin	Tangential mixing chamber	0.1x PBS	18 mM	2.3	7.4, 9.0, 10.5	SA: 10 fM (→70 aM)	[35] Reed
			Anti-IgG, anti-IgA	IgG, IgA		$NaHCO_3$	1 mM	10	8.4	< 100 fM	
8	T; p-Si, n-Si (t=40, w=50-150)	APTES	Biotin	Streptavidin	Tangential mixing chamber	1x PBS	180 mM	0.7*	7.4	Undetected	[47] Reed
						0.1x PBS	18 mM	2.3*	7.4	Observed	
						0.01x PBS	1.7 mM	7.3*	7.4	Observed	
			ssDNA: probe 1 and 2	ssDNA: target 1 and 2		.005x PBS	83 mM	3.3*	7.4	False positives at $\lambda_D > 3.3$ nm	
9	T; n-Si (t≤40)	APTES	PSA-Ab	PSA	Microfluidic	Phosphate	6 μM	130	7.6	30 aM	[42] Lee
10	T; n-Si (t≤50-80, w=5-50, l=1-1000); Pass: Si_3N_4	APTMS	ssPNA	ssDNA	Microfluidic	TE	40 mM	1.6	8.5	10 fM	[39] Kong
11	T; n-Si and p-Si (w= 20, t= ≤32, l= 30); Pass: Si_3N_4	tert-BAC	ssDNA	ssDNA	Microfluidic	1x SSC	240 mM	0.65	7.2	10 pM	[49] Heath
		APDMES								1 nM	
12	T; n-Si, p-Si (w= 50, t=60, l=20); Pass: SiO_2	MPTMS	ssDNA	ssDNA	N/A	Water (>18 MΩ)	N/A	N/A	N/A	25 pM	[46] Williams
13	T; n-Si (w=50, t=60, l=100)	NBAD	ssPNA	ssDNA	Mixing cell	0.01x SSC	2.4 mM	6.5	7.4	N/A	[48] Zhang

[a]Abbreviations—B: bottom-up fabrication technique, mainly using Si/SiO_2 as a substrate; T: top-down fabrication technique, using SOI as substrate; d: diameter (nanometer); w: width (nanometer); t: thickness (nanometer); l: length (micrometer); Sub: substrate; n-Si: n-type Si NWs; p-Si: p-type Si NWs; n-In_2O_3: n-type In_2O_3 NWs; Pass: passivation layer made of. [a9]Several NW FETs were fabricated with the following width/length (nm/μm): 67/2, 100/10, 94/10, 67/5, 141/20.

[b]Abbrevitions---APTMS: aldehyde propyltrimethoxysilane (also called 3-(trimethoxysilyl)propyl aldehyde); Biotinyl/Avidin: avidin protein intervening layer adsorbed on Si NWs functionalized using biotinyl *p*-nitrophenyl ester; 3-PPA: 3-phosphonopropionic acid; APTES: 3-aminopropyltriethoxysilane; tert-BAC: *tert*-butyl allylcarbamate; APDMES: aminopropyldimethylethoxysilane; MPTMS: 3-mercaptopropyltrimethoxysilane; NBAD: 10-*N*-boc-amino-dec-1-ene.

[c,d]Abbreviations—Ab: antibody; anti-: antibody for a specific antigen; PSA: prostate-specific antigen; CEA: carcinoembryonic antigen; Mucin-1: cell surface protein associated with carcinomas; IgG: immunoglobulin G; IgA: immunoglobulin A; ssDNA: single-stranded DNA; ssPNA: single-stranded peptide nucleic acid.

[f]Abbreviations—HEPES: buffer based on 4-(2-hydroxyethyl)-1-piperazineethanesulfonic acid, widely used in cell culture; PBS: phosphate buffered saline; TE: Tris/ethylenediaminetetraacetic acid (EDTA) buffer, useful in handling DNA or RNA solutions; SSC: saline-sodium citrate buffer, useful in hybridization experiments.

[g]*Notes*: The ionic strength was calculated using the buffer composition reported in the referenced paper using the formula: $I = 0.5x(\Sigma c_i z_i^2)$, where c_i is the concentration of the ion and z_i its charge.

[h]*Notes*: The Debye length was estimated using the formula: $\lambda_D = 0.32(I)^{-0.5}$, where I is the ionic strength of the solution. [h8]These values of Debye length were reported in the referenced paper.

[i]*Notes:* [i6,i7]($\rightarrow x$): the lowest detectable concentration of analyte could approach x.

the ready availability of SOI wafers. Top-down techniques have been the preferred method for NW production in the field of FET nanobiosensors, as readily apparent from Table I.

Nanobiosensors can be prepared using e-beam lithography, a technique that uses a beam of electrons to pattern the substrate surface, defining the width and length of the resulting NWs. The NW produced by e-beam lithography typically have width of 50 nm and lengths ranging from 20 μm up to 1 mm [35], [42], [46], [47]. A combination of deep ultraviolet lithography with a size-reduction strategy (self-limiting oxidation) was used to produce Si NW with widths smaller than e-beam NWs, ranging from 5 to 50 nm [39], [48]. Another top-down technique is the SNAP method used by Heath and coworkers [49], [50]. This method uses molecular beam epitaxy (MBE) to create a physical template for NW patterning on GaAs/AlGaAs superlattice. This pattern for NW is then transferred on a previously n- or p-doped SOI, resulting in the production of highly aligned, 20-nm-wide Si NWs.

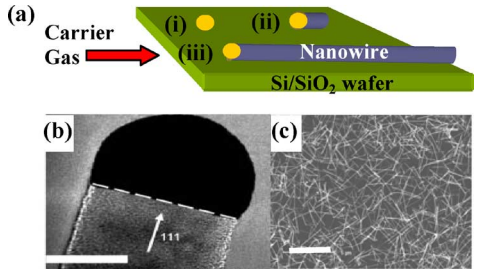

Fig. 4. Synthesis of NWs by VLS method. (a) Catalyst nanoparticles are dispersed on the Si/SiO_2 substrate (i). A liquid alloy forms when molecular precursors carried by a stream of gas initially decompose and dissolve on the catalyst nanoparticle (ii), ultimately leading to the growth of NWs (iii). (b) High-resolution TEM images of a Si NW tip grown by the VLS method. The NW retains the diameter of the catalyst (scale bar: 20 nm) and a consistent direction of growth, in this particular case, along the (1 1 1) axis. (c) Randomly oriented In_2O_3 NWs grown by laser ablation VLS at the author's facility (scale bar: 5 μm). (b) Reprinted and/or adapted with permission from [53] (IOP Publishing Ltd.: copyrights 2006).

B. Bottom-Up Technology

The bottom-up approach involves preparing NWs from molecular precursors, rather than starting with the bulk semiconductor. Bottom-up methods are used to produce both group IV semiconductor NWs and metal oxide NWs. Bottom-up techniques can be used to produce high-quality NWs; however, these NWs grow with random orientation on the substrate and are characterized by a distribution of lengths and diameters [39]. The variation in NW dimension, relative to top-down-based devices, can impose limits on bottom-up sensors because of poor device uniformity and low fabrication yields [49]. Bottom-up techniques allow the growth of NWs on a wide range of substrates, limited only by the temperature of the process used to form the NWs, which is typically in the 800–1000 °C range. The most common substrate is a Si wafer; however, the choice of substrates can be expanded to low-temperature materials by growing the NWs on a thermally stable substrate and transferring them to a second, less thermally stable substrate, such as plastic or glass [51]. NWs produced by bottom-up techniques for use in nanobiosensing can be grouped into two main synthetic approaches: vapor–liquid–solid (VLS) synthesis and laser ablation VLS.

During VLS, NWs are synthesised in an "atom by atom" fashion. Catalyst nanoparticles are uniformly dispersed on the substrate, as shown in Fig. 4(a–i). A stream of carrier gas, containing the NW molecular precursors, is flowed over the substrate at elevated temperatures. These precursors (for instance, SiH_4 to make Si NWs) initially decompose on the catalyst nanoparticle and dissolve the molten catalyst, forming an alloy in liquid state (ii). Continuous decomposition of the gas-phase precursors ultimately saturates the catalyst particle and the semiconductor precipitates, leading to the NW growth (iii) with a random orientation on the substrate surface, as shown in Fig. 4(c). The catalyst defines the diameter of the growing NWs, which will retain the same diameter as the catalyst nanoparticle, as shown in Fig. 4(b). An advantage of the VLS method is the possibility to selectively dope the growing NWs by adding dopant precursor to the carrier gas to prepare p-type or n-type NWs. For example, 20-nm-diameter Si NWs were produced by a VLS method using gold nanoclusters as a catalyst and diborane or phosphine as dopant precursors to prepare p-type or n-type NWs, respectively [52], [53]. The NWs were then transferred to a fresh silicon substrate and aligned using a flow-directed technique, resulting in a uniform, parallel NW array.

A variation of the VLS method described before uses laser ablation to evaporate the semiconducting material and is especially useful for NWs that cannot be prepared from volatile precursor compounds. We have used this method to prepare indium oxide NWs [54]–[56]. The substrate preparation is very similar to that of the VLS method, with catalyst nanoparticles dispersed on the substrate. A laser is used to vaporize the desired precursor material, which is then transported by the carrier gas to the substrate, where NWs are grown by the VLS method described before [57]. The In_2O_3 NWs have diameters typically of 10 nm and also grow with random orientation on the substrate, as shown in Fig. 4(c).

IV. Fabrication of NW FETs

Once the NWs have been prepared, the source, drain, and gate electrodes are deposited to complete the structure of the FET. At this stage of the fabrication process, some important parameters can be defined, such as the channel length (distance between the source and the drain), channel width (length of the source and the drain), and the type of electrode passivation. In all of the Si- and In_2O_3-based bionanosensors reported to date, the silicon substrate serves as the gate electrode. These parameters are illustrated in Fig. 2(a) and (b). The device dimensionality directly affects the response time [43]. The kinetics of sensing, as a function of FET dimensions, has been simulated theoretically by Sheehan and Whitman [58]. They found that the channel length is the critical dimension for analyte accumulation on the NW surface, since the sensitivity is a function of the total analyte flux over the sensing wire. According to their simulations, fabricating FET devices with longer channel lengths will significantly decrease the time required to produce a signal at a

given concentration of analyte [58]. A compromise has to be reached with regards to the best channel length. Long channel lengths are desirable from a kinetic point of view but not from an electronic point of view, where longer NWs are known to be less sensitive [45]. A common channel length is on the order of 2–10 μm.

Source and drain electrodes are usually vacuum-deposited onto a patterned surface. A thin adhesion layer of a metal is typically employed to anchor 50- to 100-nm-thick Au [35], [36], [47], [57], [59], [60], Pt [49], or Ni [21], [59], [61] electrodes to SiO_2 surfaces. Common adhesive metal layers consist of 5–50 nm of Ti [46], [49], [57], [60], [62], Cr [35], [47], [48], [59], and Al [35], [46], [47]. Source and drain electrodes are then often protected by a passivation layer in order to avoid complications during measurements, such as corrosion, electrochemical reactions or change in metal work function due to nonspecific binding of analytes. Passivation is often achieved by deposition of a Si_3N_4 layer for the entire device except on the NW sensing region and contact pads [21], [39], [49], [52], [61].

V. Surface Chemistry: Attaching a Capture Agent to the NW Surface

Although the NW FETs described above will be sensitive to the surrounding environment, they will not have the desired molecular recognition properties. The surface of the sensing element (NW) needs to be modified so that the device acquires specific recognition toward a desired analyte. This selectivity is typically achieved by anchoring a specific recognition group to the surface of the NW. A bifunctional linker molecule with two chemically different termini is used to help anchor the receptor molecules to the NW surface. Linker molecules and receptors used for sensing studies are summarized in Table I. In the case of Si NWs, the linker molecule of choice depends on whether or not the wire has an oxide coating. In the case of metal oxide NWs, a good choice for a linker molecule is the one that is terminated with a group capable of forming a nonhydrolizable conjugate, such as siloxides or phosphonates. Fig. 5 shows such a process for some representative molecules used to functionalize different types of surfaces. After covalent attachment of the receptor molecules, unreacted sites are usually deactivated with other highly reactive molecules, such as ethanolamine, butyl amine, or 2-mercaptoethanol.

A. Functionalization of Si NWs Coated With a Native Oxide Layer

A variety of linker molecules have been designed to bind to the native oxide coating the Si NWs. Alkoxysilane derivatives are the most widely used linkers. The Si-methoxide or Si-ethoxide reacts with the surface OH group, anchoring the linker molecule to the silicon oxide surface. A very common linker for Si/SiO_2 NW functionalization is 3-(trimethoxysilyl)propyl aldehyde (APTMS). The functionalization procedure involving the use of APTMS is shown in Fig. 5(a). This linker produces an aldehyde-rich surface that can be directly used to covalently immobilize monoclonal antibodies [21], [60], [61],

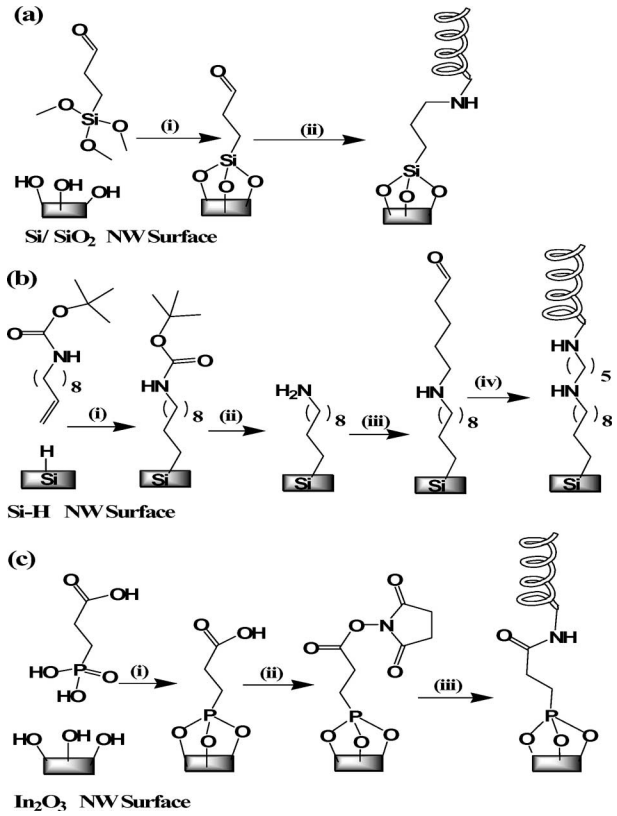

Fig. 5. Chemical pathways used to anchor biological molecules to different nanomaterial surfaces. (a) Surface of a Si/SiO_2 NW reacts with alkoxysilane derivatives, such as APTMS (i) providing an aldehyde-terminated surface. Biomolecules can then be covalent immobilized to these aldehyde groups via a coupling reaction (ii). (b) UV-mediated hydrosilylation of a Si–H surface in the presence of an olefin such as 10-N-Boc-amino-dec-1-ene (ii) followed by trifluoroacetic acid deprotection (ii) coating the Si NWs with amino groups. Activation of such a surface with glutaraldheyde (iii) facilitates the covalent attachment of biomolecules (iv). (c) Phosphonate derivatives such as 3-PPA can be immobilized to an In_2O_3 surface by simple deposition from aqueous solutions. Biomolecules can be attached upon activation of the carboxylic residue with coupling reagents such as N-(3-dimethylaminopropyl)-N'-ethylcarbodiimide (EDC)/N-hydroxysuccinimide (NHS) (iii).

amino-terminated peptide nucleic acids (PNA) [39], and DNA oligonucleotides [21].

Another popular linker molecule is 3-aminopropyltriethoxysilane (APTES). This reagent yields a surface coated with amino groups. These $-NH_2$ groups can be activated toward bioconjugation by using the proper coupling reagent. For instance, Kim *et al.* used glutaraldehyde to produce a surface that is reactive toward amine groups present in the chemical structure of the monoclonal antibody prostate-specific antigen (PSA) in order to immobilize the receptor on the surface [42]. In other studies, APTES was used to immobilize biotin [47], calmodulin [36], or oligonucleotides [47]. A thiol-terminated surface was produced upon reaction with 3-mercaptopropyltrimethoxysilane (MPTMS). This –SH terminus was then used to immobilize DNA probes modified with acrylic phosphoramidite at the 5′-end [46]. Even if widely used as linkers, the propensity of trialkoxysilanes to form multilayers can significantly affect future device performances. In fact, a consistent increase in thickness of the NW was observed

with increasing reaction time, due to the growth of a siloxane glass layer on the NW surface. These thicker NWs showed significant decrease in the device sensitivity [19]. In order to avoid this multilayer formation, monoalkoxysilanes can be used in lieu of trialkoxysilanes. For instance, the amino group of 3-aminopropyldimethylethoxysilane was used to physically adsorb DNA single strands on the NW surface [49]. Hahm and Lieber immobilized biotinyl p-nitrophenyl ester on the NW followed by a layer of avidin. Next, biotin-terminated PNA was adsorbed on this avidin layer, resulting in the attachment of PNA to the NW surface [62]. This method placed the receptor molecule distant from the sensing surface.

B. Functionalization of H-Terminated Si NW Surfaces

The native (1–2 nm thick) surface oxide on Si NWs may limit sensor performance due to the presence of interfacial electronic states [63], [64]. In addition, the surface SiO_2 acts as a dielectric that can screen the NWs from the electric field of the analyte. The silicon oxide coating can be easily etched away, for instance, by submerging the NWs into dilute HF. This replaces the native oxide layer with a hydride-terminated silicon surface. This hydride-terminated surface was found to be air-stable for several days [65]. The Si–H bond can be rapidly photodissociated with UV light to generate radical species on the Si surface. These radicals can subsequently react with terminal olefin groups on linker molecules, thus forming stable Si–C bonds at the Si surface. This photochemical hydrosilylation treatment selectively functionalizes the Si NWs, but does not react with the underlying SiO_2 layer of the substrate [66], as shown by X-ray photoelectron spectroscopy (XPS) analysis [49]. This photohydrosilylation treatment carried out using an olefin derivative of an easily cleavable carbamate, followed by deprotection, results in Si NWs coated with amino groups, as shown in Fig. 5(b). The $-NH_2$ groups can then be used to physically adsorb probe single-stranded (ssDNA) on the Si NWs [49], and attach several biotin derivatives, antibodies [35], and probe ssPNA [48].

C. Functionalization of Metal Oxide NWs

In the case of metal oxide NWs, the optimum linker molecule was found to be a phosphonate derivative [57], [67], like 3-phosphonopropanoic acid [57], as shown in Fig. 5(c). This phosphonate binds strongly to the NW surface from aqueous solutions or polar solvents. Activation of the carboxylic group enabled PSA antibody to be attached to the linker bound to the surface of In_2O_3 NWs [57].

VI. Measurements Setup

A. Buffers Used for Real-Time Detection of Analytes

During sensing measurements, biological analytes need to be delivered to the nanosensor surface. These analytes are usually dissolved in aqueous buffers, preferably at a pH and electrolyte concentration similar to that of physiological solution. Phosphate buffered saline (PBS) is a good model for human serum, which, like PBS, has a pH value of 7.40 and 0.15 M electrolyte. The pH and especially the electrolyte concentration are critical experimental variables to be considered.

Computational models for the response time of a nanobiosensor in a diffusion-capture regime were examined by Nair and Alam in order to study the effects of electrostatic screening caused by buffer solutions [44]. Their calculations predict that the sensor response varies linearly with pH and logarithmically with electrolyte concentration. Their simulation is in good agreement with data available in the literature, which indeed show that nano-FET sensors respond linearly to pH variation (which is crucial for protein detection) but nonlinearly to electrolyte concentration. Thus, they suggest developing analyte-binding schemes at low ionic strength, in order to reduce the time taken to obtain a detectable signal change. However, such a scheme might present problems related to the necessity of meeting certain minimum electrolyte concentrations in order to retain a strong binding affinity between probes and target molecules (*vide infra*).

An important parameter that influences the device performance is the Debye length (λ_{D}). The Debye length is defined as the maximum distance at which an external charge can influence the NW carrier concentration [45]. The value of Debye length (in nanometers) in water can be calculated with good approximation using the formula $\lambda_{\mathrm{D}} = 0.32(I)^{-1/2}$, where I is the ionic strength of the buffer solution [68]. Aqueous media used in the studies reviewed here, along with their ionic strength, calculated λ_{D} and pH, are summarized in Table I. In aqueous media, the accumulation of carriers inside the NW occurs over a depth equal to λ_{D}; however, the Debye length decreases rapidly with an increase in the ionic strength [41]. Probe molecules must therefore be attached as close as possible to the NW surface, yet still retain their biological activity. The Debye length plays an important role during immunological experiments where "large," relatively-low-charged biomolecules, such as antibodies, capture their target proteins. When operating at the electrolyte concentration of serum, the Debye length ($\sim$0.7 nm) is much smaller than the size of many antibodies (ca., 10–15 nm) and many proteins (ca., 5–10 nm). Therefore, at such a short λ_{D}, the electrolytes present in the buffer screen the charges carried by the analyte, as shown in Fig. 6(a), resulting in a smaller NW conductance change. Decreasing the salt concentration in the analyte solution allows for detection of larger biomolecules. At longer Debye lengths, charged residues on the analyte located several nanometers away from the NW will still exert an effect on the charge carriers in the NW, as shown in Fig. 6(b) and (c). One way to ensure longer Debye lengths is to use dilute buffer solutions with low electrolyte concentrations. However, this practice could be problematic due to complications caused by the necessary dilutions when preparing the sample. A second problem with excessive dilutions is the fact that a minimum salt concentration is necessary to retain biological activity of some proteins and is indispensable for DNA hybridization [41].

To demonstrate the effect of the Debye length on the nanosensor sensitivity, Stern *et al.* used the well-studied biotin–streptavidin (SA) couple. Binding of this ligand–receptor system was monitored with p-type Si NW FET sensors using different

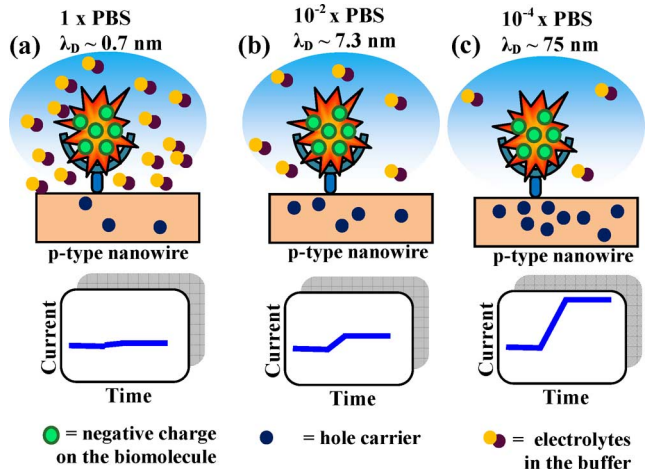

Fig. 6. Effect of the buffer electrolyte concentration on the sensitivity of NW-based FET sensors shown for a p-type NW device and a negatively charged analyte molecule. (a) At high electrolyte concentration (1× PBS, short Debye length), most of the charge carried by the captured analyte is screened by ions present in the buffer. This screening causes the analyte charge to have little effect on the accumulation phenomena that would provide an increase of the device conductance. (b) Operating at a lower electrolyte concentration (0.01× PBS), the charge carried by the analyte is poorly screened, and thus, a larger change in conductance can be observed. (c) In very dilute buffers, charges located far away from the wire can still exert an influence on the carrier density of the wire, resulting in extreme sensitivities.

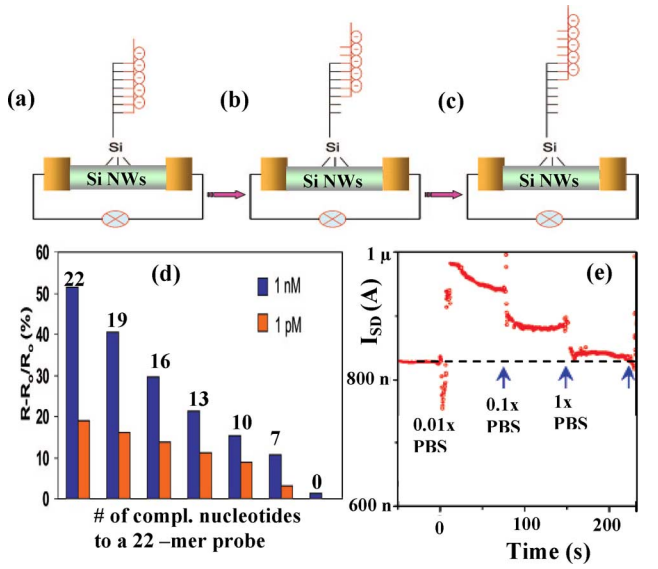

Fig. 7. Dependence of the device sensitivity as a function NW–analyte distance or buffer ionic strength. (a)–(c) Schematic showing the strategy used to place the DNA analyte charge at a fixed distance from the NW surface. (d) Sensitivity of the device, which used a PNA probe, is reported as a function of the number of complementary nucleotide present in the target DNA sequence. For fully complementary DNA, the device exhibited the greatest sensitivity. The device became progressively less sensitive as the number of mismatched nucleotides increased and the bound portion of the DNA moved away from the NW surface. (e) Influence of the electrolyte concentration on device sensitivity investigated using a biotin–SA system. As the Debye length decreased by going from 0.01× to 1× PBS, the ability of the NW device to sense the presence of bound SA decreased as well. (a)–(d) Reprinted and/or adapted with permission from [46] (Copyright 2004 American Chemical Society) and (e) from [47] (Copyright 2007 American Chemical Society).

buffer ionic strengths, but at constant SA concentration [47]. This system is ideal for this study, as the biotin–SA binding affinity is known to be unaffected by variations in buffer salt concentrations [47]. A stable baseline signal was established with biotin immobilized on the NW surface in 0.01× PBS buffer ($\lambda_D \sim 7.3$ nm), as shown in Fig. 7(e). Addition of 10 nM SA in the same buffer caused the negatively charged SA to bind to the biotinylated device and increased conductance with respect to baseline. These results imply that the majority of the protein's charge is unscreened and thus influences the carrier density in the NW. When the buffer ionic strength was increased tenfold ($\lambda_D \sim 2.3$ nm), the protein's charge was partially screened by the stronger buffer and the conductance decreased due to a weaker chemical gating effect of the bound SA. A further tenfold increase (now, 1× PBS, $\lambda_D \sim 0.7$ nm) screened most of the protein's charge, leading to a negligible change in device conductance with respect to the initial baseline. A parallel experiment with a nonbiotinylated device showed no response. This experiment clearly demonstrates that the electrolyte concentration of buffers is a critical variable influencing the sensitivity of these nanobiosensors. This sensitivity dependence on the buffer composition is an important limitation for future applications of nanobiosensors when fast detection is required. Other immunological assays based on optical detection, such as enzyme-linked immunosorbent assay (ELISA), can comfortably operate at serum's electrolyte concentrations. In the Stern *et al.*'s study, it was demonstrated that by carefully choosing λ_D, it is possible to operate in such a way that only bound analytes would produce a signal while the presence of unbound molecules is screened, thus significantly reducing false positive results. For instance, at 0.05× PBS, DNA-modified devices[1] were shown to respond only to the target DNA and be insensitive to nontarget DNA, whereas in more dilute buffers, false positives were observed.

The relationship between the spatial location of charge and chemical gating effects was also investigated by Zhang *et al.* [48]. They used the hybridization of ssDNA to a ssPNA probe immobilized on the NW surface, at constant buffer ionic strength (constant λ_D) and fixed length of DNA (constant DNA charge). The only variable was the number of complementary DNA bases with respect to the PNA receptor. This number changed from fully complementary (22 nucleotides) to noncomplementary by decreasing three bases at a time. Using this strategy, the distance of the charge layer produced by the bound target DNA to the Si NW surface was varied by controlling the location of the hybridization sites, as illustrated in Fig. 7(a)–(c). The PNA–DNA hybrid and partial hybrid were assumed to stand normal to the NW surface. As the complementary segment became shorter and the DNA charge layer moved away from the nanosensor surface, the ability of the NW device to signal the hybridized DNA was progressively diminished [Fig. 7(d)]. These results confirm that the detection sensitivity of NW devices is strongly dependent on the location and strength of the electric field produced by analyte molecules on the NW surface.

[1]Many other experimental conditions reported in the referenced paper need to be taken into consideration.

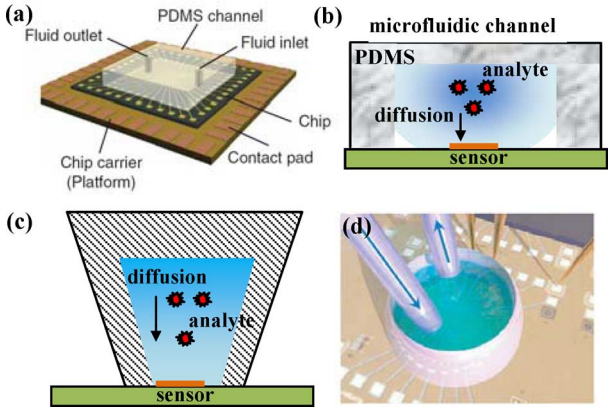

Fig. 8. Delivery systems. (a) Microfluidic channels can be used to precisely deliver a small volume of analyte above the NW sensor. (b) View along the flow direction. The flux inside the microfluidic channel is higher in the central part of the channel. The analyte has then to diffuse perpendicularly to the flux in order to reach the sensor surface. (c) Alternatively, a mixing cell (or solution chamber) can be used for analyte delivery. A mixing cell usually consists of a cone-shaped device with a narrow bottom aperture. A sensor is placed underneath in contact with the analyte solution through this small window. The analyte diffuses to the sensor surface unless (d) a system with injection and drain valves facilitate the analyte transport. (a) and (d) Reprinted and/or adapted with permission from [59] (Macmillan Publisher Ltd.: Nature Protocols, copyright 2006) and [35] (Macmillan Publisher Ltd.: Nature, copyright 2007), respectively.

B. Analyte Solution Delivery

Another important factor to be taken into consideration is the system used to deliver the analyte solution. The analyte must reach the active sensing surface in order to interact with the capture agent. The time a receptor takes to capture its target molecule is affected by the delivery strategy. Since fast responses are highly desirable, rapid analyte delivery is crucial to the development of nanobiosensors. So far, two main methods have been utilized for such a delivery: microfluidic channels [21], [36], [39], [42], [49], [59]–[62] and mixing cells [35], [46]–[48], [57], each having its advantages and disadvantages.

A microfluidic channel is usually made of molded elastomer such as polydimethylsiloxane (PDMS) with injection and drain channels, as shown in Fig. 8(a). The microfluidic devices are placed on the top of the nanosensor so that the solution can be directed over the NWs. A key benefit of a microfluidic device is that it allows the analysis to be conducted using exceedingly small samples, on the order of a nanoliter. The flow within the central part of the channel is laminar and has a higher flux than at the periphery. When a sample is injected into the channel, in order for the analyte to reach the sensor surface, the analyte has to diffuse normal to the flow, from the middle of the channel to the bottom where the NWs are located [Fig. 8(b)]. Laminar microfluidic flow thus partially restricts the ability of molecules to reach the nanosensor surface [58], especially for molecules with high molecular weights (above 100 kDa) that are known to diffuse an order of magnitude slower than smaller biomolecules such as oligonucleotides [58]. Several computational models of the sensing phenomena suggest that the analyte delivery to the sensor surface might be the limiting step toward the detection of analytes at ultralow concentrations [45], [58]. Simulations indicate that limits imposed by analyte transport in microfluidic systems will prevent nanoscale sensors from reaching detection in the femtomolar range, for assays performed in minutes, unless novel methods to actively direct biomolecules to a sensor surface are developed. Also, another disadvantage of PDMS channels is caused by the highly hydrophobic sidewalls present in these devices. Hydrophobic biomolecules with low solubility in buffers are likely to adsorb and deposit along the PDMS walls. A passivation strategy, using the protein repelling properties of polyethylene glycol, was developed by Wang *et al.*, thus reducing undesirable, nonspecific adsorption of biomolecules [60].

The other popular delivery method, shown schematically in Fig. 8(c), utilizes a mixing cell (also called solution chamber). This cell, typically a cone-shaped, plastic sample holder, is placed over the nanosensor chip and allows the solution to be delivered from the top aperture. For simple cells, where there is no continuous flow, different solutions are delivered by replacement methods and the analyte diffuses isotropically until it reaches the sensor surface. A more advanced mixing cell setup, shown in Fig. 8(d), has been designed by Stern *et al.* [35]. In this setup, injection of the solution tangential to the NW-FET sensor significantly decreased the detection response times compared to those observed in NW-FETs that used microchannels for the detection of similar target molecules [49], [62].

VII. Real-Time, Electrical Detection of Analytes

Oligonucleotides and proteins are the two main biologically relevant species detected with NW FET nanobiosensors. However, NW FET devices can also be utilized to monitor the activity of potential drug molecules [60] or detect the presence of large biological entities such as viruses [61]. Analytes used in the works reviewed here are summarized in Table I along with device performances.

A. Detection Using DNA-Modified FET Nanosensors

The detection of specific sequences of nucleic acids is very important from a clinical diagnostic point of view in order to recognize particular base sequences known to be associated with cancer or other diseases. The strong molecular charge of the DNA backbone is expected to produce a significant electric field, which should strongly affect the conductivity of the NWs. A traditional approach to DNA detection utilizes a ssDNA probe (attached to the NW) that can hybridize with its complementary single strand. This strategy requires a minimum 10 mM of electrolyte concentration at room temperature to ensure robust hybridization [45]. Operating at such high salt concentration could significantly diminish the device sensitivity. Therefore, using a different probe/capture molecule such as the uncharged PNAs offers several advantages over DNA probes. First, PNA–DNA can hybridize at low electrolyte concentrations, conditions under which there is a long Debye length and the devices are expected to be particularly sensitive. Second, ssPNA offers the potential to hybridize either a ssDNA or a DNA duplex [69], although the latter has yet to be reported for a nanobiosensor. Third, a recent report [39] revealed that by using a PNA probe,

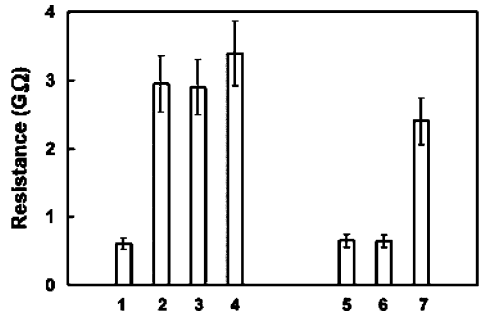

Fig. 9. Resistance of a Si NW FET after surface treatments with either DNA or PNA. A blank Si NW (1) functionalized with DNA capture probes (2) resulted in a significant increment in resistance. Upon hybridization with 1.0-nM complementary PNA, the device characteristics remained unchanged (3), whereas a 14% increase in resistance was observed upon hybridization with 1.0-nM complementary DNA (4). A similar Si NW device (5) modified with PNA capture probes (6) did not show any chance in resistance. In sharp contrast, hybridization of (6) with 1.0 nM complementary DNA led to a significant increase in resistance (7). Reprinted and/or adapted with permission from [39] (Copyright 2007 American Chemical Society).

it was easier to detect an incoming DNA strand because of the neutral background offered by PNA. In this study, the change in resistance was compared for Si NW devices immobilized with either ssDNA or ssPNA probes, as shown in Fig. 9. Immobilization of only the probe DNA produced a resistance increase of greater than 300%, whereas for the PNA probe, the resistance of the device was unchanged. Upon hybridization with complementary DNA, a 14% conductance change was observed for the DNA probe as opposed to a 200% increase in resistance for the PNA modified device. However, the physics behind these observations has not been clearly elucidated, and the advantage conferred by charge neutral probes over charged probes is still an open question.

The benefits listed before have led to several investigations using PNA probes. The first example of detection using such a system was reported by Hahn and Lieber, who used a PNA probe to target a particular DNA sequence corresponding to the wild-type ΔF508 in the cystic fibrosis transmembrane conductance regulator (CFTR) gene [62]. The functionalization strategy used in this experiment placed the probe PNA at a significant distance from the sensing surface, approximately corresponding to the size of the avidin protein. The buffer composition and ionic strength were not mentioned in this experiment; thus, the value of the Debye length is unknown. Even with a layer of avidin coating the NWs, the device showed remarkable sensing capabilities. Hybridization with 60 fM target DNA produced a strong signal in relatively short time (less than 10 s), and this sensor demonstrated a limit of detection (LOD) of 10 fM. Control experiments with noncomplementary DNA did not show a signal, proving that sequence specificity key to genetic-based disease detection [19].

A PNA capture probe was also the choice of Gao *et al.*, who demonstrated the possibility of detecting ssDNA in roughly 40 mM concentration of electrolytes [39]. Concentration dependence studies reveal that the p-type Si NW devices had an increase in conductance of about 250% in 60 min when a solution of 1 nM target DNA was used, as shown by curve 4 in Fig. 10(a). When a buffer solution was flowed over the sensor, the device did not show any appreciable change after 60 min, indicating the robustness of hybridization taking place at $\sim$40 mM ionic strength. The same experiment established a detection limit of 10 fM for target DNA when operating with a $\lambda_{\mathrm{D}} \sim 1.6$ nm. The specificity of the sensor device was also studied using ssDNA with mismatched nucleotides placed in the middle of the ssDNA sequence. A target DNA strand with a single mismatch decreased the response signal by 85% relative to fully complementary target DNA, whereas a DNA strand with two mismatches gave a 96% decrease, as shown by curves 2 and 3 in Fig. 10(b). A DNA strand with three mismatched oligonucleotides did not produce any binding signal.

The ability to detect DNA at electrolyte concentrations comparable to physiological media was demonstrated for the first time by Bunimovich *et al.* [49]. In fact, the detection of a 16-mer DNA was observed in buffer with 240 mM ionic strength. The authors used a noncovalent method to immobilize the captured ssDNA to the NWs. In their strategy, probe ssDNA was physically adsorbed to the amino-modified NW surface by electrostatic interactions, resulting in the oligonucleotides lying flat for the full length on the NWs. The advantage of this method is that, upon hybridization, the probe–target DNA duplex will also lay flat on the NWs. Thus, at $\lambda_{\mathrm{D}} \sim 0.7$ nm, the full DNA duplex was probably within the Debye length, which is crucial for high sensitivity. Moreover, in this study, the difference in sensitivity between Si NWs with and without the native oxide layer were reported and compared for the first time in the nanobiosensing literature. When the SiO_2 layer was significantly reduced, the device LOD was 10 pM; a two-order-of-magnitude improvement compared to Si NWs coated by their native SiO_2 (LOD $=$ 1 nM), as shown in Fig. 10(c) and (d). The authors also noted that their attempt to carry out hybridization in pure water resulted in no changes in Si NW resistance; thus, noncomplementary DNA gave no response. Such low LOD at very short λ_{D} could be the result of a combination of relatively low NW dimensions (Table I, entry 11) and surface functionalization strategies, which removed the Si native oxide.

The complementary detection of ssDNA was demonstrated by Li *et al.*, using both p- and n-type Si NWs [46]. Interestingly, the authors chose a 25 pM solution of target DNA as analyte in pure water. The devices response was fast, less than 50 s, as revealed from their published data shown in Fig. 10(e) and (f). This proves that extremely low electrolyte concentrations allow shorter response times. This is the first study to report DNA–DNA detection in pure water, in sharp contrast to work from other authors [49]. Device responses are shown in Fig. 10(e) for a p-type NW where a 46% increase in conductance took place (accumulation mode) and Fig. 10(f) for an n-type with 12% decrease in conductance (depletion mode).

The binding of the enzyme telomerase to nucleotides and further biological activity was monitored using an FET nanosensor modified with a 24-mer oligonucleotide [21]. This enzyme binds to eukariotic chromosomes and adds a specific nucleotide sequence (TTAGGG) to the 3′-end of DNA strands in the chromosomes. The mechanism of this binding/addition is illustrated

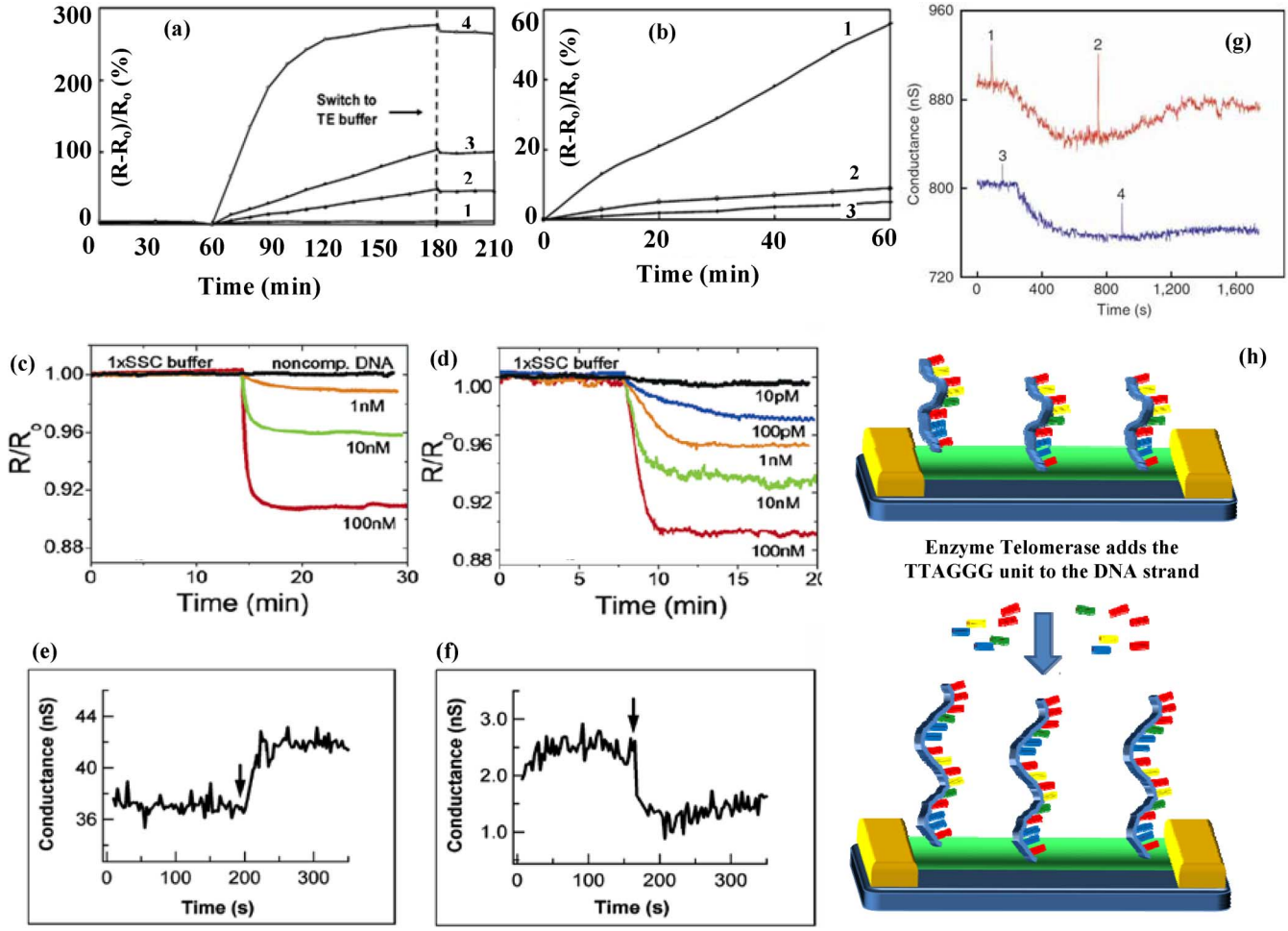

Fig. 10. Different experiments utilizing a nucleic acid probe. (a) Concentration dependence studies monitoring the change in resistance of the PNA-modified Si NW versus time in the presence of (1) 1.0-nM control, (2) 25 fM, (3) 100 fM, and (4) 1.0 nM target DNA. Specificity of the device was determined using mismatched target DNA. (b) Detection data showed that one-base mismatched (2) and two-base mismatched (3) target DNA result in 85% and 96% less signal, respectively, than if fully complementary target DNA (1) is used. The difference in sensitivity when the surface of two identical devices was functionalized using two different strategies: (c) native oxide layer was present on the Si NWs; (d) Si NWs with reduced surface oxide layer. The latter exhibited a two-orders-of-magnitude improvement for the detection of DNA. Complementary detection of 25 pM target DNA solution in pure water using a p-type NW (e) and an n-type NW (f). The arrow indicates the point in time when the DNA was added. (g) Conductance versus time data recorded for oligonucleotide-modified p-type silicon NW devices (1) after the introduction of a solution containing telomerase as extract from 100 HeLa cells and 0.4 mM dCTP, (2) a mixture of desoxynucleic acids triphosphate (dNTPs) (dATP, dGTP, dUTP, and dCTP) each at 0.1 mM, (4) 0.4 mM dCTP only. (h) Telomerase, upon binding to a DNA single strand immobilized to the Si NWs surface, catalyzes the addition of the telomeric repeat sequence TTAGGG to the end of chromosomes when in the presence of deoxynucleotode triphosphates. (a)–(b), (c)–(d), (e)–(f), and (g) were reprinted and/or adapted with permission from [39] (Copyright 2007 American Chemical Society), [49] (Copyright 2006 American Chemical Society), [46] (Copyright 2004 American Chemical Society), and [21] (Macmillan Publisher Ltd.: Nature Biotechnology, copyright 2005), respectively.

in Fig. 10(h). Telomerase was present in the fluid extracted from HeLa cells, which was diluted in buffer and injected into the microfluidic channel to reach the sensor device. At physiological pH, telomerase (pI $\sim$ 10) is positively charged; upon binding to the DNA probe, telomerase caused a decrease in the device conductance, as shown in Fig. 10(g) (points 1 and 3). The biological activity of telomerase was retained even when bound to the Si NW surface. In fact, upon the addition of deoxynucleotide triphosphates (point 2), telomerase incorporated the TTAGGG sequence into probe DNA. A stronger negative charge on the probe caused the device conductance to increase. Interestingly, telomerase binding could be observed without amplification from the amount of fluid extracted from just ten cells.

B. Detection Using Immunologically Modified FET Nanosensors

Proteins are another important class of biomolecule that can be detected using such NW FETs. Cancer-derived proteins or existing proteins present at abnormal concentration are biomarkers that can be tracked to monitor the progress of cancer. Therefore, devices that can quantify the level of biomarkers in serum or other human samples have potential application in the diagnosis of cancer or other diseases. However, when developing an immunological nanobiosensor platform, experiments involving the well-understood and inexpensive probe–target pairs such as biotin–SA or biotin–avidin are usually carried out at the initial stages. Then, as the research progresses, the detection of more desirable, health-care-related biomolecules,

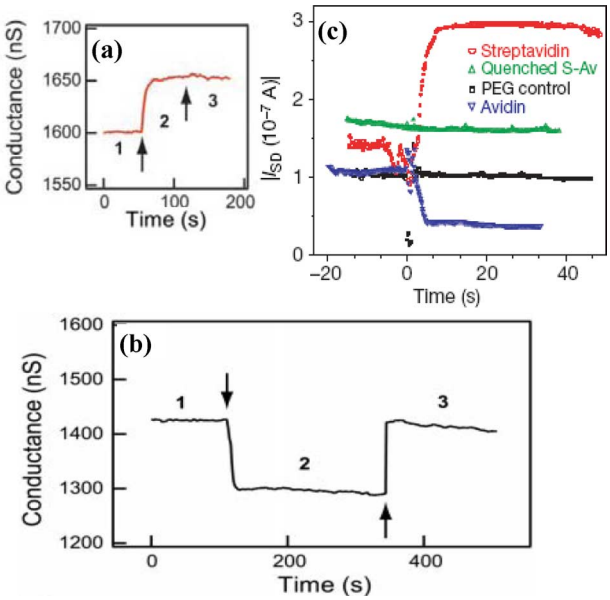

Fig. 11. Detection studies using biotin as a capture probe. (a) Plot of conductance versus time for analyte detection using biotin-modified Si NWs. Region 1 corresponds to buffer solution, region 2 to the addition of 250 nM SA, and region 3 to pure buffer solution. (b) Conductance versus time for a biotin-modified Si NW. Region 1 corresponds to buffer solution, region 2 to the addition of 3 μM antibiotin, and region 3 to the flow of buffer solution. (c) Specific recognition and charge determination of SA and avidin using p-type Si NWs. (a)–(b) and (c) were reprinted and/or adapted with permission from [36] (Copyrights: AAAS, 2001) and [35] (Macmillan Publisher Ltd.: Nature, copyright 2007), respectively.

such as cancer biomarkers or viruses, can be implemented. In fact, the first example of a real-time, electrical detection of a protein from a solution using a FET nanosensor, reported by Cui *et al*. in 2001, used the biotin–SA probe–receptor complex [36]. The interaction of biotin and SA was monitored using p-type Si NWs, and binding was observed with an LOD of 10 pM of SA, at $\lambda_D \sim 3.4$ nm. The conductance of the NW device increased rapidly, in agreement with the gating effect of the negatively charged SA [Fig. 11(a)]. Upon addition of pure buffer, the signal remained stable because of the high binding affinity between biotin and SA (Fig. 11(a), region 3). A system with lower binding affinity than biotin–SA, biotin–antibiotin (monoclonal antibody), was then chosen to prove reversible binding and regeneration of the sensing surface. As expected, the flow of fresh buffer rapidly removed the bound antibiotin and the device conductivity returned back to baseline, suggesting successful recovery of the sensor [Fig. 11(b)].

Other research groups have used biotin as a receptor during the development of sensing platforms. Also, the very different pI of SA ($\sim$5) and avidin ($\sim$10) offer the possibility to observe a complementary type of response for a given device. For instance, Stern *et al*. reported that interaction of positively charged avidin decreased the conductance of a p-type NW device, as shown in Fig. 11(c) [35]. In contrast, the conductance increased when negatively charged SA was used as an analyte. This behavior demonstrates that the sensing mechanism truly depends on chemical gating effects. The experimental conditions used in this paper ($\lambda_D \sim 2.2$ nm, pH $= 7.4$) are similar to those used by Lieber's group ($\lambda_D \sim 3.4$ nm, pH $= 9$) for the same analyte (SA) [36], thus allowing a comparison of the two sensing platforms. Lieber's group reported an LOD of 10 pM, whereas Stern's report demonstrated a potential LOD at 70 aM. Even though Cui *et al.* worked with a more dilute buffer at higher pH (which gives a higher net negative charge to SA) and smaller NWs (20 nm by VLS synthesis), the platform used by Stern *et al.* showed over five orders of magnitude higher sensitivity. The difference in sensitivity might come from both fabrication strategies and experimental conditions. Factors to be considered include density of doping, surface functionalization strategy (which may significantly reduce the native oxide) and employment of a specially designed cell to inject the solution tangential to the NWs (see Section VI-B).

Several cancer biomarkers (antigens) have been detected using antibodies as receptors on the NW surface. Devices fabricated using either p- or n- type Si NWs were used by Zheng *et al*. to detect several cancer biomarkers such as PSA, carcinoembryonic antigen (CEA), and mucin-1 [21]. These biomarkers were analyzed either individually or in a mixture using a multiplexed detection scheme. For detection of PSA, a more extensive analysis was conducted using a number of different experiments. First, a linear device response to the PSA concentration was observed in the range 1.4 nM to 2.6 fM, with an LOD of 2 fM, when the buffer media had a $\lambda_D \sim 130$ nm [Fig. 12(a)]. Second, the negatively charged PSA induced a complementary response when either a p- or an n-type Si NW device was used, as shown in Fig. 12(b). This complementary response confirms that carrier depletion or accumulation is the mechanism behind the change in conductance for these devices. Third, detection of PSA was tested against a background of proteins in high concentration (total protein: 59 mg/mL). A PSA sample was made by mixing a buffer solution with either human or donkey desalted serum. NW devices were capable of detecting PSA from such a complex sample with an LOD of 26 fM, an analyte "concentration $\sim$ 100 billion lower than that of background serum proteins." The other cancer biomarkers were detected from model solutions with similar sensitivity: CEA had an LOD of 0.55 fM and mucin-1 of 0.49 fM ($\lambda_D \sim 130$ nm). A multiplexed detection scheme was also demonstrated when the three cancer biomarkers were detected simultaneously using three parallel, independent p-type Si NW FETs. Buffer solutions containing PSA, CEA, or mucin-1 were sequentially delivered over the sensors. Each one of these FETs was designed to detect one specific biomarker by functionalizing its surface with the corresponding antibody [Fig. 13(a)]. The results of this experiment are shown in Fig. 13(b). Clearly, only the expected sensor responded to the analyte, while the other two sensors showed no response, demonstrating the selectivity necessary to incorporate these Si NW FETs into large array of devices with the potential to simultaneously analyze complex biological samples, such as blood serum.

The detection of the cancer biomarker PSA has also been demonstrated by several other research groups. For example, PSA was used as analyte by Kim *et al.* to investigate the influence of FET dimensionality (channel width and length) and doping concentrations on the device sensitivity [42]. Lightly doped

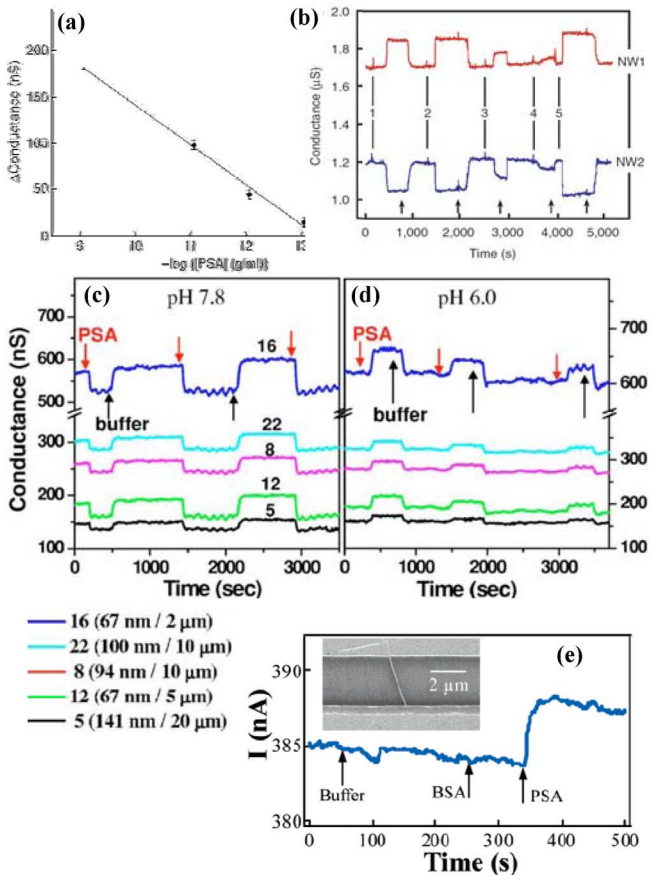

Fig. 12. (a) Change in conductance versus concentration of PSA for a p-type Si NWs modified with PSA–Ab receptor. The device response is proportional to the analyte concentration in the range 5 ng/mL to 90 fg/mL and the lower detection limit was 2 fM. (b) Complementary sensing of PSA using p-type and n-type NW devices. Vertical lines correspond to the addition of PSA solution of (1) and (2) 0.9 ng/ml, (3) 9 pg/ml, (4) 0.9 pg/ml, and (5) 5 ng/ml. Complementary detection of PSA using n-type Si NWs at two different pH values: (c) 7.8 and (d) 6.0. For both (c) and (d), each curve represents a NW with a different configuration (channel length/width): 16 (67 nm/2 μm), 22 (100 nm/10 μm), 8 (94 nm/10 μm), 12 (67 nm/5 μm), and 5 (141 nm/20 μm). (e) Current recorded over time for an individual In_2O_3 NW device when sequentially exposed to buffer, BSA, and PSA. (Inset) SEM image of the single NW device used for this detection. (a), (b), (c)–(d), and (e) were reprinted and/or adapted with permission from [21] (Macmillan Publisher Ltd.: Nature Biotechnology, copyright 2005), [59] (Macmillan Publisher Ltd.: Nature Protocols, copyright 2006), [42] (Copyrights 2007, American Institute of Physics), and [57] (Copyright 2005 American Chemical Society), respectively.

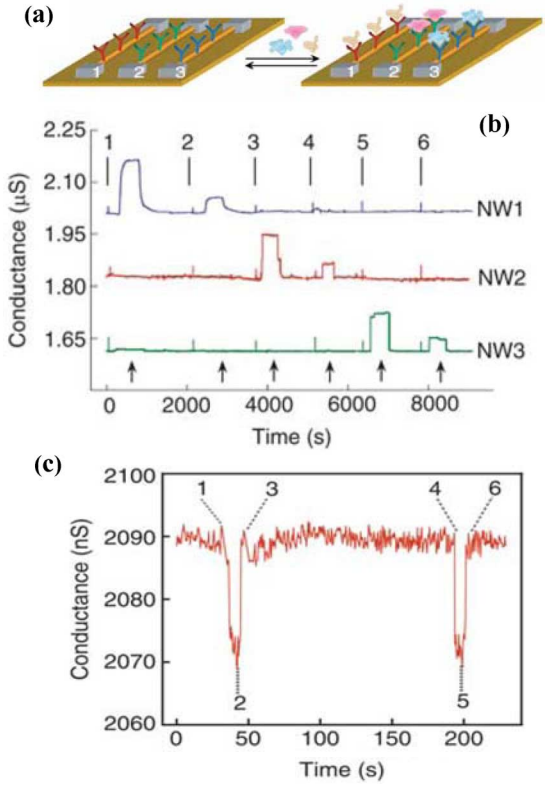

Fig. 13. Some challenging experiments such as multiplexing or detection of a virus. (a) Schematic illustration of multiplexed detection of cancer biomarkers. Three parallel, independent p-type Si NW FETs, NW1, NW2, and NW3 were functionalized with anti-PSA, anti-CEA, and anti-mucin-1, respectively. Multiplexed data are shown in (b). Solutions of analytes were delivered to the NW array sequentially as follows: (1) 0.9 ng/ml PSA; (2) 1.4 pg/ml PSA; (3) 0.2 ng/ml CEA; (4) 2 pg/ml CEA; (5) 0.5 ng/ml mucin-1; and (6) 5 pg/mL mucin-1. Clearly, only the device designed to respond to the analyte injected showed a response; the other two showed no response. Buffer solutions were injected following each protein solution at points indicated by black arrows. (c) Conductance vs. time for a single silicon NW device after introduction of influenza A solution containing 100 viral particles/μL. (a) and (b)–(c) were reprinted and/or adapted with permission from [21] (Macmillan Publisher Ltd.: Nature Protocols, copyright 2006) and [18] (reproduced with permission of the *MRS Bulletin*), respectively.

devices, with a channel conductance below 500 nS, showed the highest sensitivity in good agreement with other recent reports [43]–[45]. The high resistance could be achieved by either controlling the device dimensions (longer length and narrow width) or by varying the doping density. Kim's study also reported the detection of PSA using n-type NW FETs, with 30 aM analyte solutions ($\lambda_D \sim 130$ nm) adjusted to different pHs. The pH values were chosen to be above (pH $= 7.8$) and below (pH $= 6.0$) the isoelectric point of PSA (pI ~ 6.9). Adjusting the pH values above or below pI of PSA causes the analyte to assume an opposite overall charge so that the n-type NW devices would show divergent responses for the two solutions [Fig. 12(c) and (d)]. The conductance of the NWs increased with PSA binding at pH $= 7.8$ and decreased with PSA binding at a pH of 6.0. Data are also given for devices with different channel dimensions in Fig. 12. The device with the smallest channel dimensionalities gave the highest sensitivity, as expected. In these figures, each curve represents the response from an FET with different dimensions (see entry 9 in Table I). The specificity toward PSA was tested using a 10^9-fold higher concentration of BSA in the background. In theory, the devices reported in this paper could approach detection in single-digit attomolar concentrations of PSA, the highest sensitivity reported to date for label-free, immunologically FET nanobiosensing.

In order to use these nanobiosensors for the analysis of real samples or even for *in vivo* application, the devices need to operate at high electrolyte concentrations. Our group has demonstrated that PSA can be detected at electrolyte concentrations similar to physiological media. Our platform was based on a single, n-type indium oxide NW FET, as shown in the inset of Fig. 12(e) [57]. To the best of our knowledge, this is the only example of NW-based FET sensor that uses a material other

than silicon. The PSA antibody immobilized on the surface was able to capture the PSA protein (140 pM) in 1× PBS buffer, with room to push the LOD down to 7 pM. This was the first time that antibody/antigen detection was reported in such high electrolyte concentration. The In_2O_3 NWs exhibited superior performance when employed as chemical sensors operating in dry conditions [70]–[73]. Efficient sensing was also observed when operating in an aqueous environment even under nonideal conditions. In fact, in this experiment, PSA sensing was carried out at a pH very close to the protein pI resulting in a low, net overall charge (pH = 7.4). Also, the undiluted PBS buffer resulted in a very short λ_D (∼0.8 nm) that could have screened most of the charge on the protein. Observation of a binding signal under such conditions is in disagreement with [35], where 1× PBS screened the electric field produced by the captured SA. The discrepancy can be explained by the fact that our In_2O_3 NWs ($d = 10$ nm) have a much higher S/V ratio than the Si NWs used in [47] ($w = 50$–150 nm and $t = 40$ nm) and thus, are much more sensitive.

Other examples of antibody–antigen detection performed under conditions closer to physiological serum was reported by Stern *et al*. Mouse immunoglobulin G (IgG) and mouse immunoglobulin A (IgA) were detected with good selectivity at 100 fM antigen concentration [35]. These low LODs at high electrolyte concentration might be due to the surface functionalization and analyte delivery strategies employed in the devices. The native oxide layer on the Si NWs was significantly reduced, and a specially designed cell was employed to inject the solution tangential to the NWs (see Section VI-B).

The next logical step once the antibody–antigen recognition and detection by NWs has been demonstrated is the detection of larger biological entities expressing a surface protein that can be specifically recognized by a receptor antibody. Viruses and their corresponding antibodies are ideal candidates for such experiments. The detection of a virus (influenza A) was first reported by Patolsky *et al*. using an NW device functionalized with the corresponding antibody, anti-hemagglutinin [61]. The viruses diffuse in solution while the signal is stable at baseline, as shown by point 1 in Fig. 13(c). Binding of the virus causes a drop in conductance (point 2), which returns to the baseline once the virus is released. Multiple virus binding/release events were observed, as shown by points 4–6. Selectivity toward a particular virus and multiplexing were also demonstrated using a multiple device array. Two sets of NW were functionalized with the antibodies for influenza A virus and adenovirus, respectively. Upon sequential delivery of solutions containing either the influenza A virus, the adenovirus or a mixture of both, the response observed from the NW array was specific to the corresponding virus in the analyte solution.

C. Application of Immunologically Modified FET Nanosensors in Drug Discovery

NW-based sensing can also be employed to monitor the activity of potential drug molecules. In this application, a protein or enzyme is anchored to the NW, and the sensor is used to determine if the addition of a given drug prevents or retards the action of the protein. A good example of this drug discovery application has been reported for the protein tyrosine kinase, which is responsible for phosphorylation of tyrosine. Tyrosine kinase first binds tyrosine, then coordinates a molecule of ATP, which is later transferred to tyrosine. The binding of ATP to tyrosine kinase is a crucial step for this phosphorylation reaction. If this binding is inhibited, then phosphorylation of tyrosine will not take place. Several small molecules have been designed to bind to tyrosine kinase, preventing ATP binding. The activity of potential pharmaceuticals can thus be evaluated by NW-based sensors, as demonstrated by Wang *et al*. [60]. ATP possesses a high negative charge, and its presence can be measured easily by an NW, whereas the drug molecules tested here, such as Gleevec, are uncharged and would give no signal on binding. The structures of several other drug molecules is shown in Fig. 14(c). Binding of ATP (held at fixed concentration, 240 nM) as a function of Gleevec concentration was monitored by the NW sensor, as shown in Fig. 14(a). As Gleevec inhibits the binding of ATP to the modified NWs, the conductance of the device decreases as a function of Gleevec concentration. This concentration dependence was also used to calculate the ATP dissociation constant and drug-molecule inhibition constants. The same concept was then applied for three other drug candidates, as shown in Fig. 14(c). This method demonstrates the possibility to characterize the activity of potential pharmaceuticals in a relatively short period of time. Further developing such a platform could make NW sensors an essential tool in drug discovery.

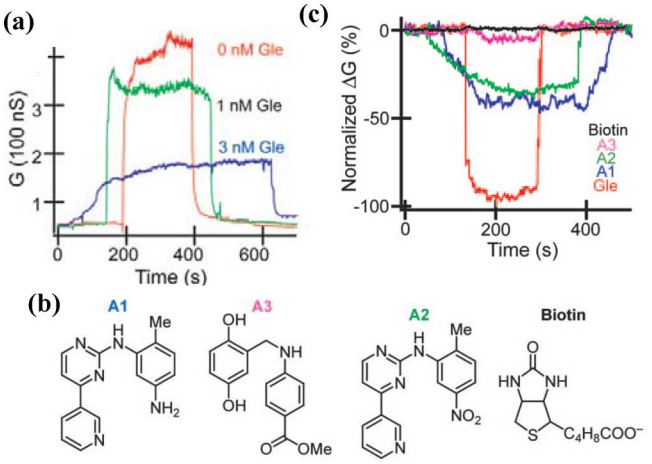

Fig. 14. Application of NW sensors to drug discovery. (a) Binding of ATP to tyrosine kinase modified NWs in the presence of different concentrations of Gleevec (Gle) is shown as conductance vs. time. The ATP concentration was fixed at 240 nM in the three experiments; the Gleevec concentrations in the solutions are indicated in the figure. ATP binding to modified NWs can be inhibited by potential drug molecules with structures shown in (b). (c) Inhibition data shown as normalized conductance vs. time for 50 nM small molecule solutions of Gleevec (red), A1 (blue), A2 (green), A3 (pink), and biotin (black) recorded in the presence of 100 nM ATP. Reprinted and/or adapted with permission from [60] (Copyright 2005 National Academy of Science, USA).

VIII. Summary

We have provided a review on the current status of FET sensors that utilize NWs as their detection element. This field of

technology is expanding rapidly and has already demonstrated several potential applications, including health monitoring and drug discovery. The devices reviewed here show high sensitivity, selectivity and short response times. Moreover, the field of nanobiosensors is young, so there is ample room for improvement. In spite of the large variety of semiconducting NW materials already employed as chemical sensors, only two types of materials have been used to fabricate biological sensors, i.e., silicon and indium oxide.

NWs produced by top-down technologies are uniform in size and can be readily integrated into electrical readout circuits; however, this technique is mostly applied to the fabrication of Si NWs because of the maturity of the necessary technology to process Si and the readily availability of SOI substrates. Also, top-down NWs usually have a much smaller S/V ratio than NWs synthesized by VLS. The approach taken by Kong's group, which combines deep UV photolithography with the self-limiting oxidation technique, is a step forward toward the fabrication of small diameter, uniform, and well-aligned Si NW sensors. The native oxide layer coating the Si NWs can affect the polarization effects induced by bound analytes. Methods that can significantly reduce the surface oxide layer have been developed using photochemical hydrosilylation of H–Si in the presence of an olefin. The NWs modified by this method showed a two-order-of-magnitude improvement in sensitivity with respect to Si/SiO_2 NWs. Other materials, such as indium oxide, do not present such a surface oxide problem, and their surface modification can be easily achieved using phosphonate derivatives using simple deposition from aqueous solutions.

When it comes to choice of the capture agents, a distinction needs to be made between the two main classes of analyte usually detected with nanobiosensors. When the detection of a particular DNA sequence is desired, PNA probes have been shown to give much more sensitive devices than ssDNA-modified devices. When the analyte is a protein, recognition is often achieved by placing the corresponding antibody on the NW surface. Antibodies, while highly specific toward the analyte recognition, are very "delicate," and their biological activity can be easily suppressed, necessitating careful handling of the device. On the other hand, aptamers offer very similar affinity for the same analyte, and at the same time, are much more robust and smaller in size. Sensing using aptamer-modified sensors, while demonstrated with CNT devices [74], has not yet been reported for NW devices.

The solutions used to deliver the analyte to the NW FET biosensors differ significantly between laboratories and literature reports. The buffer/solution composition, pH and ionic strength, ranging from highly pure water to buffers modeling blood serum, have all been used. Performance and sensitivities for these devices reported by different research groups are consequently often difficult to compare. Here, we suggest toward standardization in the field of nanobiosensors by proposing to unify the media in which detection of analytes is performed. We propose that, whenever possible, the collection data would be carried out at pH $= 7.40$ and at ionic strengths of 180, 18, and 1.8 mM, corresponding to about $1\times$, $0.1\times$, and $0.01\times$ PBS, along with other conditions specifically chosen to meet certain binding requirements. Also, data analysis requires some degree of unification as well. We propose to report device performance as a ratio of change in resistance over initial resistance ($\Delta R/R_o$) on the vertical axis and time on the horizontal axis. The $\Delta R/R_o$ ratio, also called relative response, will compensate for any device-to-device variation within a large array of devices. These steps toward standardization in the field should allow comparison between the performance of different devices, and thus, facilitate the progress in the development of nanobiosensors.

ACKNOWLEDGMENT

The authors are thankful to P. Djurovich for help with editing the manuscript.

REFERENCES

[1] M. M. C. Cheng, G. Cuda, Y. L. Bunimovich, M. Gaspari, J. R. Heath, H. D. Hill, C. A. Mirkin, A. J. Nijdam, R. Terracciano, T. Thundat, and M. Ferrari, "Nanotechnologies for biomolecular detection and medical diagnostics," *Curr. Opin. Chem. Biol.*, vol. 10, pp. 11–19, 2006.

[2] M. Ferrari, "Cancer nanotechnology: Opportunities and challenges," *Nature Rev. Cancer*, vol. 5, pp. 161–171, 2005.

[3] J. R. Heath and M. E. Davis, "Nanotechnology and cancer," *Annu. Rev. Med.*, vol. 59, pp. 251–265, 2008.

[4] F. M. Raymo and I. Yildiz, "Luminescent chemosensors based on semiconductor quantum dots," *Phys. Chem. Chem. Phys.*, vol. 9, pp. 2036–2043, 2007.

[5] N. C. Tansil and Z. Q. Gao, "Nanoparticles in biomolecular detection," *Nano Today*, vol. 1, pp. 28–37, 2006.

[6] N. L. Rosi and C. A. Mirkin, "Nanostructures in biodiagnostics," *Chem. Rev.*, vol. 105, pp. 1547–1562, 2005.

[7] X. G. Liang and S. Y. Chou, "Nanogap detector inside nanofluidic channel for fast real-time label-free DNA analysis," *Nano Lett.*, vol. 8, pp. 1472–1476, 2008.

[8] Y. Chen, X. Wang, M. K. Hong, S. Erramilli, P. Mohanty, and C. Rosenberg, "Nanoscale field effect transistor for biomolecular signal amplification," *Appl. Phys. Lett.*, vol. 91, pp. 243511-1–243511-4, 2007.

[9] P. A. Neff, A. Serr, B. K. Wunderlich, and A. R. Bausch, "Label-free electrical determination of trypsin activity by a silicon-on-insulator based thin film resistor," *Chemphyschem*, vol. 8, pp. 2133–2137, 2007.

[10] B. S. Kang, H. T. Wang, T. P. Lele, Y. Tseng, F. Ren, S. J. Pearton, J. W. Johnson, P. Rajagopal, J. C. Roberts, E. L. Piner, and K. J. Linthicum, "Prostate specific antigen detection using AlGaN/GaN high electron mobility transistors," *Appl. Phys. Lett.*, vol. 91, pp. 112106-1–112106-3, 2007.

[11] X. J. Huang and Y. K. Choi, "Chemical sensors based on nanostructured materials," *Sens. Actuators B, Chem.*, vol. 122, pp. 659–671, 2007.

[12] I. Y. Park, Z. Y. Li, X. M. Li, A. P. Pisano, and R. S. Williams, "Towards the silicon nanowire-based sensor for intracellular biochemical detection," *Biosens. Bioelectron.*, vol. 22, pp. 2065–2070, 2007.

[13] A. Poghossian, S. Ingebrandt, M. H. Abouzar, and M. J. Schoning, "Label-free detection of charged macromolecules by using a field-effect-based sensor platform: Experiments and possible mechanisms of signal generation," *Appl. Phys. A, Mater. Sci. Process.*, vol. 87, pp. 517–524, 2007.

[14] S. Ingebrandt and A. Offenhausser, "Label-free detection of DNA using field-effect transistors," *Phys. Status Solidi A, Appl. Mater. Sci.*, vol. 203, pp. 3399–3411, 2006.

[15] P. A. Neff, B. K. Wunderlich, S. Q. Lud, and A. R. Bausch, "Silicon-on-insulator based thin film resistors for quantitative biosensing applications," *Phys. Status Solidi A, Appl. Mater. Sci.*, vol. 203, pp. 3417–3423, 2006.

[16] Y. Han, A. Offenhausser, and S. Ingebrandt, "Detection of DNA hybridization by a field-effect transistor with covalently attached catcher molecules," *Surf. Interface Anal.*, vol. 38, pp. 176–181, 2006.

[17] S. Q. Lud, M. G. Nikolaides, I. Haase, M. Fischer, and A. R. Bausch, "Field effect of screened charges: Electrical detection of peptides and proteins by a thin-film resistor," *Chemphyschem*, vol. 7, pp. 379–384, 2006.

[18] F. Patolsky, B. P. Timko, G. F. Zheng, and C. M. Lieber, "Nanowire-based nanoelectronic devices in the life sciences," *MRS Bull.*, vol. 32, pp. 142–149, 2007.
[19] F. Patolsky, G. Zheng, and C. M. Lieber, "Nanowire sensors for medicine and the life sciences," *Nanomedicine*, vol. 1, pp. 51–65, 2006.
[20] F. Patolsky, G. F. Zheng, and C. M. Lieber, "Nanowire-based biosensors," *Anal. Chem.*, vol. 78, pp. 4260–4269, 2006.
[21] G. F. Zheng, F. Patolsky, Y. Cui, W. U. Wang, and C. M. Lieber, "Multiplexed electrical detection of cancer markers with nanowire sensor arrays," *Nature Biotechnol.*, vol. 23, pp. 1294–1301, 2005.
[22] S. N. Kim, J. F. Rusling, and F. Papadimitrakopoulos, "Carbon nanotubes for electronic and electrochemical detection of biomolecules," *Adv. Mater.*, vol. 19, pp. 3214–3228, 2007.
[23] K. Balasubramanian and M. Burghard, "Biosensors based on carbon nanotubes," *Anal. Bioanal. Chem.*, vol. 385, pp. 452–468, 2006.
[24] B. L. Allen, P. D. Kichambare, and A. Star, "Carbon nanotube field-effect-transistor-based biosensors," *Adv. Mater.*, vol. 19, pp. 1439–1451, 2007.
[25] G. Gruner, "Carbon nanotube transistors for biosensing applications," *Anal. Bioanal. Chem.*, vol. 384, pp. 322–335, 2006.
[26] T. Uno, H. Tabata, and T. Kawai, "Peptide-nucleic acid-modified ion-sensitive field-effect transistor-based biosensor for direct detection of DNA hybridization," *Anal. Chem.*, vol. 79, pp. 52–59, 2007.
[27] F.-S. Zhou and Q.-H. Wei, *Scaling Laws for nanoFET Sensors*. Los Alamos, NM: Los Alamos Nat. Lab., 2007, pp. 1–6, (preprint archive, condensed matter).
[28] R. A. Dubin, G. C. Callegari, J. Kohn, and A. V. Neimark, "Carbon nanotube fibers are compatible with mammalian cells and neurons," *IEEE Trans. Nanobiosci.*, vol. 7, no. 1, pp. 11–14, Mar. 2008.
[29] L. Lacerda, A. Bianco, M. Prato, and K. Kostarelos, "Carbon nanotubes as nanomedicines: From toxicology to pharmacology," *Adv. Drug Del. Rev.*, vol. 58, pp. 1460–1470, 2006.
[30] L. Lacerda, S. Raffa, M. Prato, A. Bianco, and K. Kostarelos, "Cell-penetrating CNTs for delivery of therapeutics," *Nano Today*, vol. 2, pp. 38–43, 2007.
[31] A. M. Popov, Y. E. Lozovik, S. Fiorito, and L. Yahia, "Biocompatibility and applications of carbon nanotubes in medical nano robots," *Int. J. Nanomed.*, vol. 2, pp. 361–372, 2007.
[32] M. P. Mattson, R. C. Haddon, and A. M. Rao, "Molecular functionalization of carbon nanotubes and use as substrates for neuronal growth," *J. Mol. Neurosci.*, vol. 14, pp. 175–182, 2000.
[33] R. J. Chen, H. C. Choi, S. Bangsaruntip, E. Yenilmez, X. W. Tang, Q. Wang, Y. L. Chang, and H. J. Dai, "An investigation of the mechanisms of electronic sensing of protein adsorption on carbon nanotube devices," *J. Amer. Chem. Soc.*, vol. 126, pp. 1563–1568, 2004.
[34] R. J. Chen, S. Bangsaruntip, K. A. Drouvalakis, N. W. S. Kam, M. Shim, Y. M. Li, W. Kim, P. J. Utz, and H. J. Dai, "Noncovalent functionalization of carbon nanotubes for highly specific electronic biosensors," in *Proc. Nat. Acad. Sci. USA*, vol. 100, pp. 4984–4989, 2003.
[35] E. Stern, J. F. Klemic, D. A. Routenberg, P. N. Wyrembak, D. B. Turner-Evans, A. D. Hamilton, D. A. LaVan, T. M. Fahmy, and M. A. Reed, "Label-free immunodetection with CMOS-compatible semiconducting nanowires," *Nature*, vol. 445, pp. 519–522, 2007.
[36] Y. Cui, Q. Q. Wei, H. K. Park, and C. M. Lieber, "Nanowire nanosensors for highly sensitive and selective detection of biological and chemical species," *Science*, vol. 293, pp. 1289–1292, 2001.
[37] I. Heller, A. M. Janssens, J. Mannik, E. D. Minot, S. G. Lemay, and C. Dekker, "Identifying the mechanism of biosensing with carbon nanotube transistors," *Nano Lett.*, vol. 8, pp. 591–595, 2008.
[38] X. W. Tang, S. Bansaruntip, N. Nakayama, E. Yenilmez, Y. L. Chang, and Q. Wang, "Carbon nanotube DNA sensor and sensing mechanism," *Nano Lett.*, vol. 6, pp. 1632–1636, 2006.
[39] Z. Gao, A. Agarwal, A. D. Trigg, N. Singh, C. Fang, C. H. Tung, Y. Fan, K. D. Buddharaju, and J. Kong, "Silicon nanowire arrays for label-free detection of DNA," *Anal. Chem.*, vol. 79, pp. 3291–3297, 2007.
[40] N. Elfstrom, R. Juhasz, I. Sychugov, T. Engfeldt, A. E. Karlstrom, and J. Linnros, "Surface charge sensitivity of silicon nanowires: Size dependence," *Nano Lett.*, vol. 7, pp. 2608–2612, 2007.
[41] C. Heitzinger and G. Klimeck, "Computational aspects of the three-dimensional feature-scale simulation of silicon-nanowire field-effect sensor for DNA detection," *J. Comput. Electron.*, vol. 6, pp. 387–390, 2007.
[42] A. Kim, C. S. Ah, H. Y. Yu, J. H. Yang, I. B. Baek, C. G. Ahn, C. W. Park, M. S. Jun, and S. Lee, "Ultrasensitive, label-free, and real-time immunodetection using silicon field-effect transistors," *Appl. Phys. Lett.*, vol. 91, pp. 103901-1–103901-3, 2007.
[43] P. R. Nair and M. A. Alam, "Performance limits of nanobiosensors," *Appl. Phys. Lett.*, vol. 88, pp. 233120-1–233120-3, 2006.
[44] P. R. Nair and M. A. Alam, *Screening-Limited Response of Nanobiosensors*. Los Alamos, NM: Los Alamos Nat. Lab., 2007, pp. 1–7 (preprint archive, condensed matter).
[45] P. R. Nair and M. A. Alam, "Design considerations of silicon nanowire biosensors," *IEEE Trans. Electron Devices*, vol. 54, no. 12, pp. 3400–3408, Dec. 2007.
[46] Z. Li, Y. Chen, X. Li, T. I. Kamins, K. Nauka, and R. S. Williams, "Sequence-specific label-free DNA sensors based on silicon nanowires," *Nano Lett.*, vol. 4, pp. 245–247, 2004.
[47] E. Stern, R. Wagner, F. J. Sigworth, R. Breaker, T. M. Fahmy, and M. A. Reed, "Importance of the Debye screening length on nanowire field effect transistor sensors," *Nano Lett.*, vol. 7, pp. 3405–3409, 2007.
[48] G.-J. Zhang, G. Zhang, J. H. Chua, R.-E. Chee, E. H. Wong, A. Agarwal, K. D. Buddharaju, N. Singh, Z. Gao, and N. Balasubramanian, "DNA sensing by silicon nanowire: Charge layer distance dependence," *Nano Lett.*, vol. 8, pp. 1066–1070, 2008.
[49] Y. L. Bunimovich, Y. S. Shin, W. S. Yeo, M. Amori, G. Kwong, and J. R. Heath, "Quantitative real-time measurements of DNA hybridization with alkylated nonoxidized silicon nanowires in electrolyte solution," *J. Amer. Chem. Soc.*, vol. 128, pp. 16323–16331, 2006.
[50] J. R. Heath, "Superlattice nanowire pattern transfer (SNAP)," *Acc. Chem. Res.* to be published (DOI: 10.1021/ar800015y).
[51] M. C. McAlpine, H. Ahmad, D. W. Wang, and J. R. Heath, "Highly ordered nanowire arrays on plastic substrates for ultrasensitive flexible chemical sensors," *Nature Mater.*, vol. 6, pp. 379–384, 2007.
[52] F. Patolsky, B. P. Timko, G. H. Yu, Y. Fang, A. B. Greytak, G. F. Zheng, and C. M. Lieber, "Detection, stimulation, and inhibition of neuronal signals with high-density nanowire transistor arrays," *Science*, vol. 313, pp. 1100–1104, 2006.
[53] W. Lu and C. M. Lieber, "Semiconductor nanowires," *J. Phys. D: Appl. Phys.*, vol. 39, pp. R387–R406, 2006.
[54] F. Liu, M. Bao, K. L. Wang, C. Li, B. Lei, and C. Zhou, "One-dimensional transport of In_2O_3 nanowires," *Appl. Phys. Lett.*, vol. 86, pp. 213101-1–213101-3, 2005.
[55] B. Lei, C. Li, D. Zhang, T. Tang, and C. Zhou, "Tuning electronic properties of In_2O_3 nanowires by doping control," *Appl. Phys. A, Mater. Sci. Process.*, vol. 79, pp. 439–442, 2004.
[56] C. Li, D. Zhang, S. Han, X. Liu, T. Tang, B. Lei, Z. Liu, and C. Zhou, "Synthesis, electronic properties, and applications of indium oxide nanowires," in *Molecular Electronics Iii*, vol. 1006, *Annals of the New York Academy of Sciences*, 2003, pp. 104–121.
[57] C. Li, M. Curreli, H. Lin, B. Lei, F. N. Ishikawa, R. Datar, R. J. Cote, M. E. Thompson, and C. W. Zhou, "Complementary detection of prostate-specific antigen using In(2)O(3) nanowires and carbon nanotubes," *J. Amer. Chem. Soc.*, vol. 127, pp. 12484–12485, 2005.
[58] P. E. Sheehan and L. J. Whitman, "Detection limits for nanoscale biosensors," *Nano Lett.*, vol. 5, pp. 803–807, 2005.
[59] F. Patolsky, G. Zheng, and C. M. Lieber, "Fabrication of silicon nanowire devices for ultrasensitive, label-free, real-time detection of biological and chemical species," *Nature Protocols*, vol. 1, pp. 1711–1724, 2006.
[60] W. U. Wang, C. Chen, K. H. Lin, Y. Fang, and C. M. Lieber, "Label-free detection of small-molecule–protein interactions by using nanowire nanosensors," in *Proc. Nat. Acad. Sci. USA*, 2005, vol. 102, pp. 3208–3212, 2005.
[61] F. Patolsky, G. F. Zheng, O. Hayden, M. Lakadamyali, X. W. Zhuang, and C. M. Lieber, "Electrical detection of single viruses," *Proc. Nat. Acad. Sci. USA*, vol. 101, pp. 14017–14022, 2004.
[62] J. Hahm and C. M. Lieber, "Direct ultrasensitive electrical detection of DNA and DNA sequence variations using nanowire nanosensors," *Nano Lett.*, vol. 4, pp. 51–54, 2004.
[63] T. K. Sham, S. J. Naftel, P. S. G. Kim, R. Sammynaiken, Y. H. Tang, I. Coulthard, A. Moewes, J. W. Freeland, Y. F. Hu, and S. T. Lee, "Electronic structure and optical properties of silicon nanowires: A study using X-ray excited optical luminescence and X-ray emission spectroscopy," *Phys. Rev. B*, vol. 70, pp. 045313-1–045313-8, 2004.
[64] E. Yablonovitch, D. L. Allara, C. C. Chang, T. Gmitter, and T. B. Bright, "Unusually low surface-recombination velocity on silicon and germanium surfaces," *Phys. Rev. Lett.*, vol. 57, pp. 249–252, 1986.
[65] D. D. D. Ma, C. S. Lee, F. C. K. Au, S. Y. Tong, and S. T. Lee, "Small-diameter silicon nanowire surfaces," *Science*, vol. 299, pp. 1874–1877, 2003.
[66] J. A. Streifer, H. Kim, B. M. Nichols, and R. J. Hamers, "Covalent functionalization and biomolecular recognition properties of DNA-

modified silicon nanowires," *Nanotechnology*, vol. 16, pp. 1868–1873, 2005.
[67] M. Curreli, C. Li, Y. H. Sun, B. Lei, M. A. Gundersen, M. E. Thompson, and C. W. Zhou, "Selective functionalization of In_2O_3 nanowire mat devices for biosensing applications," *J. Amer. Chem. Soc.*, vol. 127, pp. 6922–6923, 2005.
[68] K. Maehashi, T. Katsura, K. Kerman, Y. Takamura, K. Matsumoto, and E. Tamiya, "Label-free protein biosensor based on aptamer-modified carbon nanotube field-effect transistors," *Anal. Chem.*, vol. 79, pp. 782–787, 2007.
[69] F. Pellestor and P. Paulasova, "The peptide nucleic acids (PNAs): Introduction to a new class of probes for chromosomal investigation," *Chromosoma*, vol. 112, pp. 375–380, 2004.
[70] D. H. Zhang, Z. Q. Liu, C. Li, T. Tang, X. L. Liu, S. Han, B. Lei, and C. W. Zhou, "Detection of NO_2 down to ppb levels using individual and multiple In_2O_3 nanowire devices," *Nano Lett.*, vol. 4, pp. 1919–1924, 2004.
[71] C. Li, B. Lei, D. H. Zhang, X. L. Liu, S. Han, T. Tang, M. Rouhanizadeh, T. Hsiai, and C. W. Zhou, "Chemical gating of In_2O_3 nanowires by organic and biomolecules," *Appl. Phys. Lett.*, vol. 83, pp. 4014–4016, 2003.
[72] D. J. Zhang, C. Li, X. L. Liu, S. Han, T. Tang, and C. W. Zhou, "Doping dependent NH_3 sensing of indium oxide nanowires," *Appl. Phys. Lett.*, vol. 83, pp. 1845–1847, 2003.
[73] C. Li, D. H. Zhang, X. L. Liu, S. Han, T. Tang, J. Han, and C. W. Zhou, "In_2O_3 nanowires as chemical sensors," *Appl. Phys. Lett.*, vol. 82, pp. 1613–1615, 2003.
[74] H. M. So, K. Won, Y. H. Kim, B. K. Kim, B. H. Ryu, P. S. Na, H. Kim, and J. O. Lee, "Single-walled carbon nanotube biosensors using aptamers as molecular recognition elements," *J. Amer. Chem. Soc.*, vol. 127, pp. 11906–11907, 2005.

Marco Curreli received the B.Sc. degree in chemistry from California State University, Los Angeles, in 2003. He is currently working toward the Ph.D. degree in chemistry at the University of Southern California, Los Angeles.

His current research interests include the surface modification of nanomaterials and the development of nanobiosensors.

Rui Zhang received the Bachelor's degree in chemistry from Peking University, Beijing, China, in 2006. She is currently working toward the Ph.D. degree in the Department of Chemistry, University of Southern California, Los Angeles.

Her current research interests include surface modification of nanomaterials and multiplex sensing using nanobiosensors.

Fumiaki N. Ishikawa received the B.Sc. degree in chemistry and the Master's degree in energy science from Kyoto University, Kyoto, Japan, in 2002 and 2004, respectively. He is currently working toward the Ph. D. degree in materials science at the University of Southern California, Los Angeles.

His research interests include application of 1-D structured materials as nanobiosensors and transparent transistors.

Hsiao-Kang Chang received the Bachelor's degree from the Department of Electrical Engineering, National Taiwan University, Taipei, Taiwan, in 2004. He is currently working toward the Ph.D. degree in electrical engineering at the University of Southern California, Los Angeles.

His current research interests include 1-D semiconducting nanostructures and their applications.

Richard J. Cote received the Medical degree from Pritzker School of Medicine, University of Chicago, Chicago, IL.

He completed his residency at Cornell University Medical College, New York. He was a Clinical Fellow in pathology and a Research Fellow in human tumor immunology at Memorial Sloan-Kettering Cancer Center, and a Fellow in molecular pathology at New York University School of Medicine. He is currently a Professor in the Department of Pathology and the Department of Urology, Keck School of Medicine/Norris Cancer Center, University of Southern California (USC), Los Angeles, where he is also the Director of the Genitourinary Program, the Laboratory of Immunology and Molecular Pathology, and the USC Biomedical Nanoscience Initiative. His current research interests include the elucidation of cellular and molecular pathways of tumor progression, micrometastases detection and characterization, tumor suppressor gene analysis, bladder cancer, and molecular mechanisms of racial/ethnic variation and androgen independence in prostate cancer. He is also engaged in technology development, and has been involved in the development of immunohistochemical and molecular methods, such as antigen retrieval, nanoscale technologies for cancer diagnostic applications, including bionanosensors for the detection of serum tumor markers, and technologies for the capture and characterization of circulating tumor cells. He established a nanoscience program for the development of novel diagnostic platforms and targeted therapeutics at USC. He has received more than $30 million in peer-reviewed grant support, and holds numerous patents for cancer-related and nanoscale technologies. He has led three of the largest clinical trials in breast, lung, and bladder cancer, which were based on discoveries from his research. He is the author or coauthor of more than 300 publications, and is a member of numerous scientific advisory boards of both academic and industry-related institutions. He is a frequent lecturer, and is a co-editor of the standard textbooks *Immuno Microscopy: A Diagnostic Tool for the Surgical Pathologist* and *Modern Surgical Pathology*. He is the founder of several technology-based companies, including Impath, Inc., and Clarient.

Prof. Cote is listed in *Best Doctors in America* and *America's Top Doctors*. He has also been a member and an advisor to a large number of national and international study groups, cancer programs and societies, including the National Cancer Institute.

Chongwu Zhou received the B.S. degree from the University of Science and Technology of China, Hefei, China, in 1993, and the Ph.D. degree in electrical engineering from Yale University, New Haven, CT, in 1999.

He was a Postdoctoral Research Fellow at Stanford University from November 1998 to June 2000. He joined the University of Southern California (USC), Los Angeles, in September 2000. He has been involved at the forefront of nanoscience and nanotechnology, including synthesis and applications of carbon nanotubes and nanowires, biosensing, and nanotherapy.

Dr. Zhou has won a number of awards, including the National Science Foundation (NSF) CAREER Award, the National Aeronautics and Space Administration (NASA) Turning Goals Into Reality (TGiR) Award, the USC Junior Faculty Research Award, and the IEEE Nanotechnology Early Career Award. He is currently an Associate Editor for the IEEE TRANSACTIONS ON NANOTECHNOLOGY.

Mark E. Thompson received the B.S. degree in chemistry from the University of California at Berkeley, Berkeley, in 1980, and the Ph.D. degree in chemistry from California Institute of Technology, Pasadena, in 1985.

He was a Science and Engineering Research Council (SERC) Fellow in the Inorganic Chemistry Laboratory, Oxford University, for two years. In 1987, he joined the Chemistry Department, Princeton University, as an Assistant Professor. In 1995, he joined the University of Southern California, Los Angeles, where he is currently a Professor of chemistry and the Chair of the Department of Chemistry.